Fabrication of Aluminium Matrix Composites (AMCs) by Squeeze Casting Technique Using Carbon Fiber as Reinforcement

Hasan Alhashmy

A thesis submitted to the Faculty of Graduate and Postdoctoral Studies
in partial fulfillment of the requirements for the degree of

MASTER OF APPLIED SCIENCE

in Mechanical Engineering

Ottawa-Carleton Institute for Mechanical and Aerospace Engineering
University of Ottawa
Ottawa, Canada

July 2012

ABSTRACT

Composites have been developed with great success by the use of fiber reinforcements in metallic materials. Fiber reinforced metal matrices possess great potential to be the next generation of advanced composites offering many advantages compared to fiber reinforced polymers. Specific advantages include high temperature capability, superior environmental stability, better transverse modulus, shear and fatigue properties. Although many Metal Matrix Composites (MMCs) are attractive for use in different industrial applications, Aluminium Matrix Composites (AMCs) are the most used in advanced applications because they combine acceptable strength, low density, durability, machinability, availability, effectiveness and cost.

The present study focuses on the fabrication of aluminium matrix composite plates by squeeze casting using plain weave carbon fiber preform (AS4 Hexcel) as reinforcement and a matrix of wrought aluminium alloy 1235-H19. The objective is to investigate the process feasibility and resulting materials properties such as hardness at macro- and micro-scale, impact and bend strength. The properties obtained are compared with those of 6061/1235-H19 aluminium plates that were manufactured under the same fabrication conditions. The effect of fiber volume fraction on the properties is also investigated. Furthermore, the characterization of the microstructure is done using Optical Microscopy (OM) and Scanning Electron Microscopy (SEM) in order to establish relationships between the quality of the fiber/aluminium interface bond and mechanical properties of the composites.

In conclusion, aluminium matrix composite laminate plates were successfully produced. The composites show a good chemical bond between the fiber and the aluminium matrix. This bond resulted from heterogeneous precipitation of aluminium carbides (Al_4C_3) at the interface between aluminium matrix and carbon fiber. The hardness at macro- and micro-scale of the

composites increases by over 50% and the flexural modulus increases by about 55%. The toughness of the composite decreases due to the presence of brittle phases which can be improved by better oxidation prevention. Also, an optimal carbon volume fraction was observed that provides optimal properties including peak hardness, peak stiffness and peak toughness.

ACKNOWLEDGEMENT

Completing work cannot be meaningfully accomplished without our creator's assistance and peoples' help.

First of all, thanks to God almighty, all glory for his grace and enablement throughout this stage of study in my life.

I also want to express my profound gratitude to Saudi Arabia's government and the King Abdullah's Scholarship offered by the Ministry of Higher Education that gave approval for me to proceed and provided full funding.

I would like to thank my supervisor Dr. Michel Nganbe for his endless support and efforts throughout this dissertation and for his advice to me during the program.

I also want to extend my thanks to the staff of the Faculty of Graduate and Post Doctoral Studies (FGPS), and of the Mechanical Engineering Department at the University of Ottawa who provided a good environment to complete this work; special thanks to professors and the machine shop's staff for their support.

My sincere thanks to my amazing friends, office colleagues, my beloved brothers Mohammad & Hussain, and my beloved sisters Fatmah, Maryam and Keshmah for their support during my whole study.

I thank my mother Zainab Jafar Khan who faithfully supports and prays for me day and night. Without my mother, none of my successes and none of my achievements would have being possible.

I dedicate this work to my beloved late father …

TABLE OF CONTENTS

LIST OF FIGURES

LIST OF TABLES

LIST OF SYMBOLS

Symbol	Definition
α	Thermal expansion
ε_f	Flexural strain
ε	Creep rate
γ	Surface tension
θ	Contact angle
σ	Creep stress
σ_f	Fiber ultimate strength
σ_f	Flexural stress
ρ	Density
ρ_f	Fabric carbon fiber density
τ_c	Fiber/matrix bond strength or shear yield strength
A	Constant
b	Width
C_v	Coefficient of variation
d	Diameter
d	Thickness
d	Arithmetic mean of the two indentation diagonals d_1 and d_2
D	Maximum deflection of the center of the beam
E	Modulus of elasticity
E_f	Flexural modulus
F	Load
Hv	Vickers' number for hardness
I	Area moment of inertia
I_x	Second moment of area about the neutral axis x
K_i	Thermal conductivity
l	Length
l_c	Critical fiber length
M	Moment about the neutral axis
m	Slope of the initial elastic section of the load-deflection curve
n	Stress exponent
N	Number of plies
P	Property
P	Load at a given point on the load-deflection curve
Q	Activation energy
R	Gas constant
S	Standard deviation
T	Absolute temperature
y	Perpendicular distance to the neutral axis
V	Volume fraction
V_c	Composite specimen volume
w_f	Fabric carbon fiber weight
w(x)	Deflection of the neutral axis of the beam
$\bar{x}$	Mean value

1 MOTIVATION AND INTRODUCTION

1.1 Motivation

Over the past two decades, the greatest development and progress in Materials Science and Engineering research have resulted into a new generation of materials. These types of materials are called composites and contain materials of at least two different classes. There are three types of composites: Ceramic Matrix Composites (CMCs), Polymer Matrix Composite (PMCs), and Metal Matrix Composites (MMCs). There is no universal definition for MMCs from the scientists' point of view [1]. A less restrictive view of MMCs definition includes materials such as directionally solidified eutectic alloys, oxide dispersion strengthened alloys, eutectic cast alloys, pearlitic steel and two-phase lamellar alloys. A more conservative view of MMCs definition includes only materials with reinforcements that remain distinct from the matrix throughout the fabrication process [2].

A metal matrix can be reinforced with whiskers, particles, short or continuous fibers, and ceramics. Although many matrices such as lead, zinc, copper, steel, titanium and nickel have been used to form MMCs, the most research effort has been dedicated to lightweight metal alloys such as aluminium and magnesium. Light metal composites are more interesting for the aerospace industry where they offer outstanding advantages [3].

Metal matrix composites are used in a wide range of high performance applications today. The usage of MMCs was over 3.5 million kg in the year 2004 and is increasing at an annual growth rate of over 6% [4]. Most of their current applications are in aviation, ground transportation, electronics and sports industries. The applications of metal matrix composites in aeronautics have been established in the aerostructural, aeropropulsion and subsystem categories. For example, ventral fins and fuel access door covers in F-16 aircrafts; rotor blade sleeves and

swash plates in the Eurocopter EC120 and N4 helicopters; fan exit guide vanes for the Pratt and Whitney 4084, 4090 and 4098 engines used in Boeing 777. The ground transportation market has the biggest mass production of MMCs with 62% in 1999 [1]. Some major parts such as engine blocks, piston and DRA brake components, including discs, rotors, pads and caliper in the automotive and railway industries are made of MMCs. MMCs have the largest economics value in the electronics (thermal management) industry. The largest market segment for MMCs is for radio frequency (RF) microwave packaging used in telecommunication and radar systems and for conductor cables in power transmission towers. The sports market has only a limited usage for metal matrix composites such as in bicycle tubing, track spikes and lacrosse stick shafts [1].

1.2 Introduction

Composites have been developed with greater success by the use of fiber reinforcements in metallic materials [5]. Fiber reinforced metal matrices possess great potential to be the next generation of advanced composites offering many advantages compared to fiber reinforced polymers. Specific advantages include high temperature capability, superior environmental stability, better transverse, shear and fatigue properties [6]. Some potential applications of fiber reinforcement in different metal matrices are listed in Table 1.1.

Although many metal matrix composites are attractive for use in different industrial applications, aluminium matrix composites are the most used in advanced applications because they combine acceptable strength, low density, durability, machinability, availability, effectiveness and cost [1].

Table 1.1: Some applications of fiber reinforcement in different metal matrices [7].

Matrix Type	Fiber Type	Potential Applications
Aluminium	Graphite	Satellite, missile and helicopter structures
Magnesium		Space and satellite structures
Lead		Storage battery plates
Copper		Electrical contacts and bearings
Aluminium	Borsic	Jet engine fan blades
Titanium		High temperature structures and fan blades
Aluminium	Alumina	Superconductor restraints in fusion power reactors
Lead		Storage battery plates
Magnesium		Helicopter transmission structures
Aluminium	Silicon Carbide	High-temperature structures
Titanium		High-temperature structures
Superalloy		High-temperature engine components
Aluminium	Boron	Compressor blades and structure supports
Magnesium		Antennal structures
Titanium		Jet engine fan blades

The objectives of strengthening aluminium alloys are to enhance their properties such as strength, hardness, fatigue, creep, stress relaxation, corrosion, melting point, and resistance to wear [8]. There are different strengthening mechanisms that have been used in aluminium alloys industrial history; these includes solid solution, precipitation hardening, grain size reduction, strain hardening [9] and fiber reinforcement. Carbon fiber (graphite) reinforced aluminium and its alloys have been attracting a great share of research and commercial attention due to superior properties such as high temperature resistance, high strength and stiffness, lightweight, thermal and electrical conductivity, fatigue, creep and wear resistance [8,10].

Several manufacturing techniques have been used to produce aluminium matrix composites such as squeeze casting, stir casting, compo-casting, and powder metallurgy methods

[11]. Among these manufacturing techniques, squeeze casting or liquid-metal infiltration has been attracting huge interest from both the manufacturing society and the researcher community since it was found in 1960s [4]. Squeeze casting combines the advantages of traditional high-pressure die casting, gravity permanent mold die casting and common forging technology [12]. Even though squeeze casting is considered a less expensive manufacturing technique as compared to other techniques, its true and main advantages are the high quality of its products such as elimination of porosity and shrinkage, 100% casting yield, attainment of greater part details, good surface finish, good dimensional accuracy, high strength-to-weight ratio, improved wear resistance, higher corrosion resistance, higher hardness, resistance to high temperature, improved fatigue and better creep strength [5].

Manufacturing of aluminium matrix composites by squeeze casting poses several challenges such as higher processing temperatures, fiber/matrix bonding issues and the ability to produce desired geometries [12]. However, these problems are being solved and quality castings are manufactured within minimum processing time although issues remain to be solved with respect to fiber/matrix bonding, particularly in complex geometries [12,13].

The present thesis focuses on the fabrication of aluminium matrix composite plates by squeeze casting using a laminate configuration of plain weave carbon fiber fabric (AS4 Hexcel) as reinforcement and sheets of wrought aluminium alloy 1235-H19 as matrix. The objective is to investigate the process feasibility and resulting materials properties such as hardness at macro- and micro-scales, impact and bend strength. The properties obtained are compared with those of the reference 6061/1235-H19 aluminium alloy plates that were manufactured under the same fabrication conditions. The effect of fiber volume fraction on the properties is also investigated. Furthermore, the characterization of the microstructure is done using optical microscopy and

scanning electron microscopy in order to establish relationships between the quality of the fiber/aluminium interface bond and the mechanical properties of the composites. The new laminate fabrication method suggested in this thesis is expected to have the advantage of being more appropriate for fabricating gradient materials and for combining fiber and particulate/dispersion strengthening in composite materials as compared to standard squeeze casting using liquid matrix metal.

2 LITERATURE REVIEW

2.1 Mechanical properties and plastic deformation

2.1.1 Aluminium properties

Aluminium is a metallic element of atomic number 13. Its atomic weight is 26.98 amu [14]; its specific gravity is 2.7 (the ratio between the density of the aluminium and water); the crystal structure of aluminium is face-centered cubic (FCC); and the atomic radius is 0.1431 nm [14]. Aluminium is one of the easiest metals to form and has a good combination of high strength and light weight [14]. Some of the most important properties of pure aluminium are summarized in Table 2.1.

Table 2.1: Some of the most important properties of pure aluminium [14].

Properties	**Values**	**Properties**	**Values**
Melting Point	660°C	Yield Strength	35 MPa @ 20 °C
Boiling Point	2,519°C	Tensile Strength	90 MPa @ 20 °C
Density	2.71 g/mL	Ductility	Elongation = 40 % in 50 mm
Brinell Hardness	245 MPa	Elastic Modulus	69 GP @ 20 °C
Poisson Ratio	0.33	Shear Modulus	25 GP @ 20 °C

The corrosion resistance of aluminium is dependent upon a protective oxide film. This film is stable in aqueous media when the pH is between about 4.0 and 8.5. The oxide film is naturally self renewing and accidental abrasion or other mechanical damage of the surface film is rapidly repaired [15].

Conventionally, aluminium and its alloys are divided into two broad classes; castings (no forming following casting) and wrought (mechanically worked after casting). The latter is sub-divided into heat treatable and non-heat treatable alloys.

2.1.2 Dislocations and plastic deformation

Dislocations are known as one-dimensional crystallographic defects in materials at the microscopic level. The properties of the material are influenced by the presence of dislocations. Dislocations can be created when metals experience solidification, plastic deformation and thermal stresses that result from rapid cooling. Dislocations are divided principally into two types: edge and screw dislocations [8,9].

Plastic deformation can be generally defined as permanent change in shape or size of a solid material under stresses beyond its elastic limit. At microscopic level, plastic deformation at low temperature can occur by motion of a large number of dislocations within the matrix and by twinning [9]. Dislocation creep and diffusion are additional mechanisms of plastic deformation at high temperature.

2.2 Strengthening mechanisms

The objectives of strengthening aluminium alloys are to enhance strength, hardness, fatigue, creep, stress relaxation, corrosion resistance, melting point, and resistance to wear. Table 2.2 describes types of aluminium alloys and potential appropriate strengthening methods.

Table 2.2: Types of aluminium alloys and potential appropriate strengthening methods [8].

Original Matrix	Alloying	Strengthening process	Tempers
• Pure aluminium • 1xxx	• 2xxx - Cu • 6xxx - Mg, Si • 7xxx - Zn	- Solid Solution - Precipitation Hardening (Solution Heat Treatment + Natural Ageing or Artificial Ageing) - Strain Hardening (Cold Work)	Heat Treatable
	• 3xxx - Mn • 5xxx - Mg	- Solid Solution - Strain Hardening (Cold Work) - Grain Size Reduction	Non-Heat Treatable

2.2.1 Solid solution strengthening

Solid solution strengthening occurs when solute atoms are added to solvent materials (host materials). It is applied to both heat treatable and non-heat treatable alloys. Aluminium solid solution is usually substitutional where the solute (guest) atoms substitute the host atoms. The strengthening effect is due to the interaction between moving dislocations and the guest atoms, which leads to an increase in material's strength.

2.2.2 Precipitation strengthening

Precipitation hardening is caused by uniformly distributed precipitates of a second phase in a matrix material; it is achieved by appropriate heat treatments, which generally consist of solutionizing followed by ageing as illustrated in Figure 2-1. The precipitate particles behave like obstacles to dislocation movement thereby strengthening the heat treated alloys. The most common precipitation heat treated aluminium alloys are aluminium-copper alloys [8].

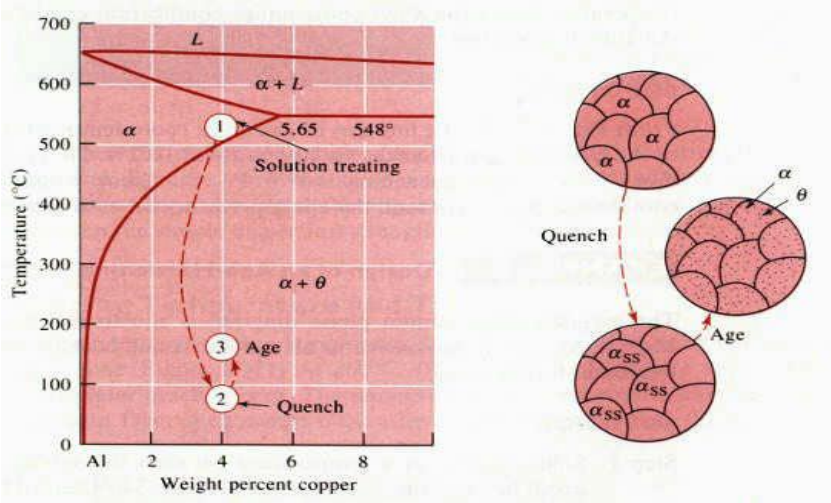

Figure 2-1: Precipitation hardening process for aluminium alloys [9].

Ageing can be divided into natural ageing and artificial ageing. Natural ageing refers to spontaneous formation of alloy structure during exposure at room temperature, which forms theta (θ) precipitate particles in the matrix. Natural ageing creates non-coherent precipitates that have no relationship with the crystal structure of the surrounding matrix as shown in Figure 2-2.a. Artificial ageing is carried out at elevated temperature to produce metastable θ' or θ'' precipitates which are coherent with the solid solution matrix as shown in Figure 2-2.b.

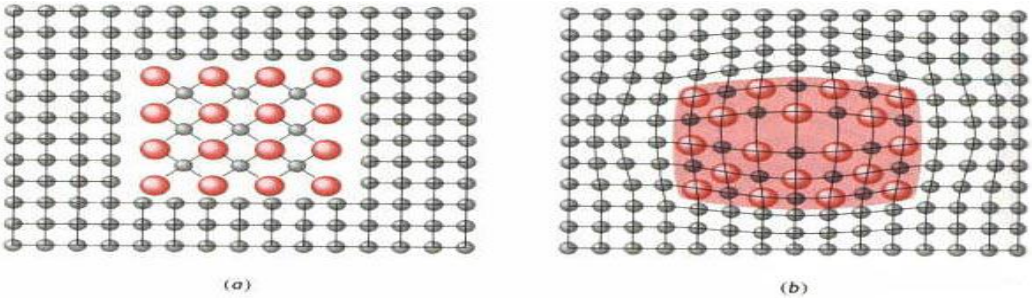

Figure 2-2: (a) Non-coherent precipitate following natural ageing, and (b) coherent precipitate following natural and artificial ageing [9].

2.3 Fiber properties and types

Fibers are filaments with at least 100:1 length-to-diameter ratio [9]. The manufacturing industry has produced different forms of fibers from the micrometer scale up to the centimeter scale. Figure 2-3 shows different scale levels of fibers. The most commonly used fibers in composites are glass, carbon/graphite, aramid/kevlar, and thermoplastic fibers [9]. This work only focuses on carbon fibers.

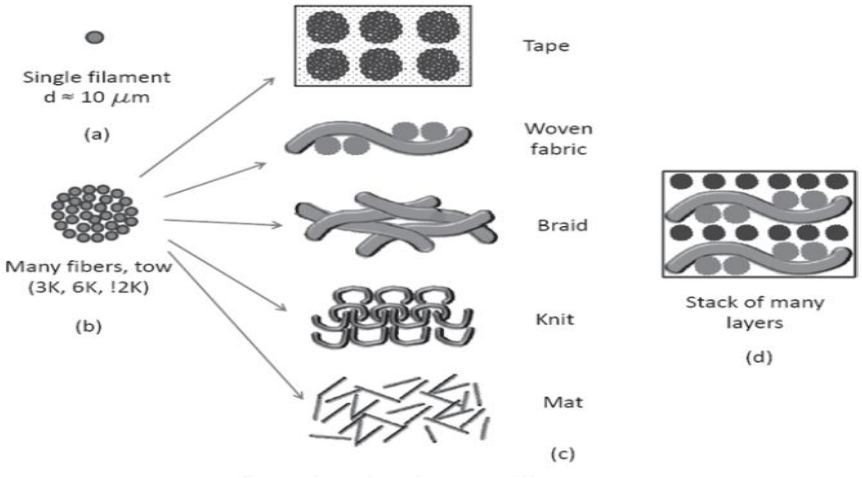

Figure 2-3: Fiber forms at different scales [16].

2.3.1 Carbon / graphite fibers

Carbon and graphite are both based on layered structures of hexagonal rings of carbon that are called graphene (true graphite). However, there is a difference between carbon and graphite fibers at least in theory. Graphite fibers are those carbon fibers that have been subjected to heat treatment at up to 1650°C, have carbon content in excess of 99%, possess 3-D ordering of the atom, and have higher tensile module [16].

2.3.2 Types of carbon fibers

Carbon fibers are made using a raw material called precursor. There are three types of carbon fibers, which are polyacrylonitrile (PAN), pitch and rayon. These types are more used in applications where mechanical properties are the priority [16,17]. This work only focuses on carbon fibers made out of PAN based precursor.

PAN based precursor: The principle of making PAN based precursor is described in Figure 2-4, which starts from polyacrylonitrile (PAN) molecules. (PAN) molecules are thermoplastic polymers made by addition of polymerization to achieve sheets of hexagons of carbon atoms [17].

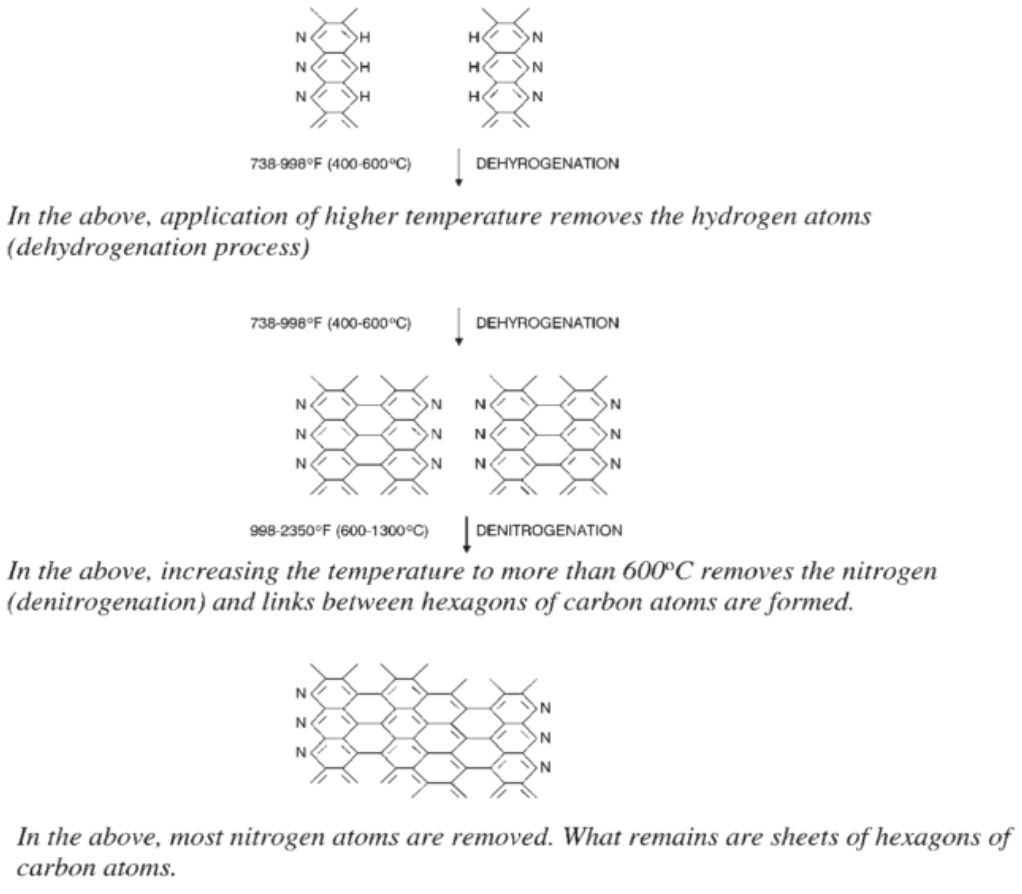

In the above, application of higher temperature removes the hydrogen atoms (dehydrogenation process)

In the above, increasing the temperature to more than 600°C removes the nitrogen (denitrogenation) and links between hexagons of carbon atoms are formed.

In the above, most nitrogen atoms are removed. What remains are sheets of hexagons of carbon atoms.

Figure 2-4: Formation of carbon fibers from PAN molecules [16].

A single fiber itself consists of many sheets of hexagons of carbon atoms. In fact, the strength and the stiffness of the fibers are based on the stiffness and the strength between the carbon-carbon bonds similar to the diamond bonds except that diamond has three bonds but a fiber has only two bonds. A microscopic cross section of a carbon fiber is shown in Figure 2-5 that shows the orthotropic configurations of carbon atoms on the fiber, arranged in the form of stack up sheets in plane direction. Post-processing of PAN based precursor is required to improve the mechanical properties of PAN characteristics such as molecular weight of carbon, carbon distribution in the stacking up sheets of the fiber, crystallinity, carbon-carbon bond diameter, molecular orientation, and impurities level [18].

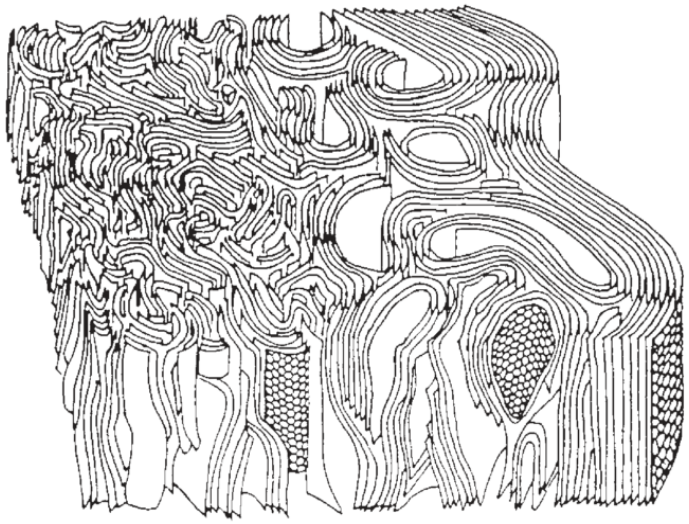

Figure 2-5: Configuration of the microscopic cross section of a carbon fiber [18].

Post-processing can be performed in different steps, which include stretching, thermosetting, carbonization and graphitization. The process starts with stretching of the fibers followed by the thermosetting step. During the thermosetting process, the PAN based precursor is first stabilized so that the polymers do not melt during subsequent processing steps. Then, the fibers are carbonized until they are essentially transformed into all-carbon fibers. At this stage, the PAN base is heated up slowly to 982°C at which approximately 94% of the carbon content is

formed with the rest being nitrogen. With further heating, the carbon content increases to 99.7%. The graphitization is achieved when the temperature exceeds 1760°C at which the tensile modulus of the fiber, the crystalline structure and the 3-D nature of the structure are improved [17].

In addition to the previous steps, the fibers are processed by surface treating and sizing to improve later bonding with the matrix and interlaminar shear strength (ILSS). Surface treatment can be divided into two types: oxidative and non-oxidative.

Oxidative treatments can be done by drawing the fibers through a bath of some appropriate oxidative agents (such as nitric acid, potassium permanganate or sodium hypochlorite), or by drawing the fiber through an acidic or alkaline electrolytic bath.

Non-oxidative treatments are of three types; whiskerization, pyrolytic surface coating, and polymer grafting. During the whiskerization process, single crystals of ceramic materials (SiC, TiO_2, or Si_3N_4) are grown on the surface of the fibers; the growth of these particles is perpendicular to the fiber axis. Both pyrolytic surface coating and polymer grafting act as bridges between the fiber and a future matrix.

In some cases, organic coatings (sizings) are also added to the fibers to further improve the fiber/matrix bonding and to protect the fibers from damage during handling. These sizings can be applied to both treated and untreated fibers by passing the fibers through a heated bath of the sizing agent. The most common sizing is an epoxy; but polyvinyl alcohol and polyimides have also been used [16].

Different approaches have been suggested for insuring best precursors of carbon fiber; the most prominent approaches include:

1. Precursors should have higher carbon content [17].

2. Precursors should be high temperature resistant, and therefore preferably an aromatic heterocyclic polymer [19].
3. There should be no more than one carbon atom between aromatic rings [19].
4. Precursor molecules should have high degree of order, orientation and flatness [20].
5. Simple release of non-carbon atoms and easy cyclization [21]; e.g., nitrogen and oxygen atoms should be a part of side groups rather than of the main chain.
6. Precursors should have a high molecular weight [17].

2.3.3 Forms of carbon fibers

There are two forms of carbon fibers: continuous and discontinuous. Carbon fibers are typically circular in cross-section and usually vary in diameter from 0.1 µm to 0.1 mm. They have specific features based on the application conditions and the matrix to be reinforced. Figure 2-6 shows different forms of carbon fiber reinforcements in a matrix [21].

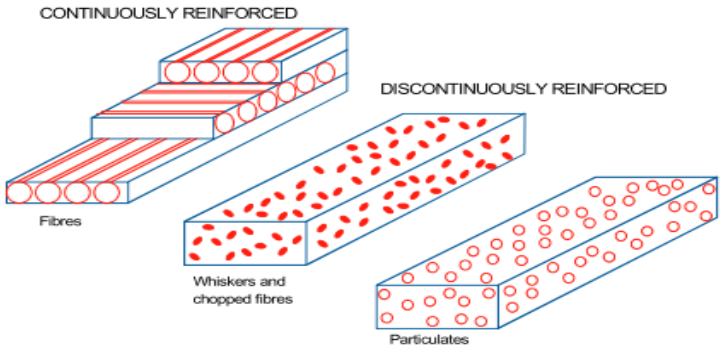

Figure 2-6: Different forms of carbon fiber reinforcement in a matrix [21].

Continuous fiber reinforced composites contain monofilaments (diameter greater than 100 µm) or tows of fibers (diameter less than 20 µm). Discontinuously reinforced composites contain short fibers, whiskers or particulates and the specific size/length of the discontinuous fibers

varies depending on the application condition, market requirement, and manufacturing procedure [22]. Table 2.3 summarizes the main features of composites reinforced using continuous and discontinuous carbon fibers respectively.

Table 2.3: Main features of composites reinforced using continuous and discontinuous carbon fibers [22].

Continuous Fibers	Discontinuous Fibers
➢ Improved stiffness & strength	➢ Strength is not the main objective
➢ Reduced wear and creep	➢ High and isotropic stiffness
➢ Anisotropic properties	➢ Almost isotropic properties
➢ Improved fatigue strength	➢ Increase in wear resistance
➢ Usually high fiber content	➢ Better controlled thermal expansion
➢ More load carried by fiber	➢ Higher service temperature

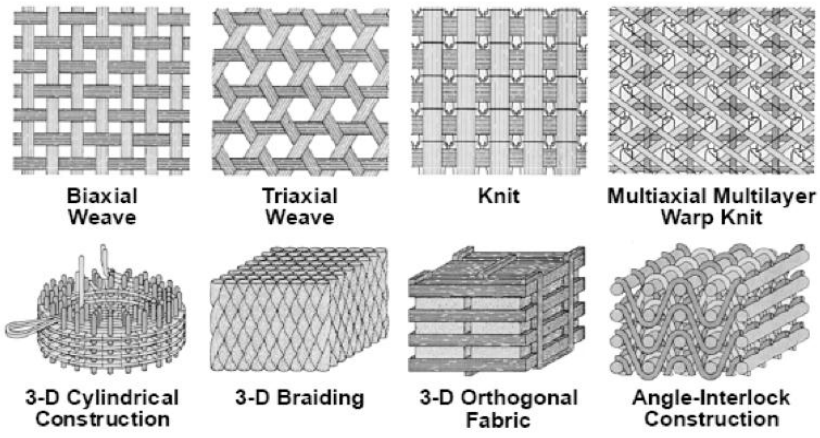

Figure 2-7: Different types of carbon fiber fabrics [16].

Continuous fibers are individual filaments that are joined together to form different types of tows and fabrics. Discontinuous fibers can also be used to form limited types of fabrics such as mats with low carbon fiber contents [22].

In fact, there are different types of fabrics classified based on the application condition and the fiber content. Layers of different fabrics can be built up to make 2D and 3D preforms as

illustrated in Figure 2-7. In this work, the most commonly used fabric textiles are used and are discussed in the next section.

2.3.4 Carbon fiber fabric textile types

1. Tows:

Tows are untwisted bundles of continuous filaments, usually with a specific count such as 3k tows (3000 filaments per tow) or 6k tows (6000 filaments per tow). Tows can be laid down as parallel fibers to form a tape. Also, they can be wound around a shape, as in filament winding, or they can be chopped into short fiber segments. A tow can also be twisted into a yarn, or several tows combined into a roving. Tows are sold on spools with a particular filament count for each tow end [16].

2. Weaves:

Woven textiles are generally made of two sets of yarns that interlace and are oriented at 90° from each another. Weaves are the strongest and most stable structures that can be obtained from interlacing yarns. Woven textiles can be 2-D or 3-D as it can be seen in Figure 2-8 that shows the basic procedure of making woven textiles [16].

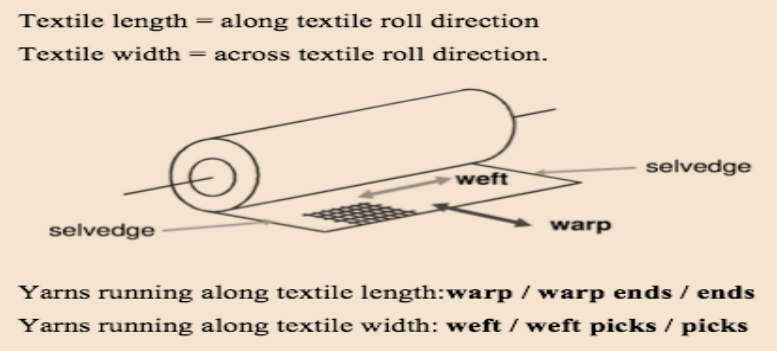

Figure 2-8: The basic procedure of making woven textile [23].

Different structures and types of woven textiles can be produced depending on required mechanical properties and application conditions. The main types of woven textiles are plain weaves, basket weaves, long shaft satin weaves or harness weaves, and tri-axial weaves [16,23].

a. Plain weave:

Plain weave is the simplest weave form. It is made by interlacing yarns in an alternating over-and-under pattern. There is one warp fiber for one fill fiber with no skipping. The maximum fabric stability and firmness with minimum yarn slippage result from this weave. The pattern gives uniform strength in two directions when yarn size and count are similar in warp and fill. This weave type is the most resistant in shear and is also considered to be a rather stiff weave. Because plain weave fabrics are stable, they are used for flat laminates.

b. Basket weave:

The basket weave is similar to the plain weave except that two warp yarns are woven one over and one under two fill yarns. This weave is less stable than the plain weave so it is more pliable. This fabric is flatter and stronger than an equivalent weight and count of plain weave. The use is similar to that of the plain weave but with better drape on mild contours.

c. Long shaft satin weave or harness weave:

The long shaft satin weave or harness weave has one warp yarn weaving over four or more fill yarns such as the 4-harness-satin weave and the 8-harness-satin weave. The long shaft satin weave is less stable than a plain weave. Also, the weave is less open than most others so wetting and air removal can be a problem unless vacuum is used. This weave is used extensively in the aircraft industry where complex shapes are common. Figure 2-9 shows different types of woven fabrics that can be hybrid or quasi uni-directional.

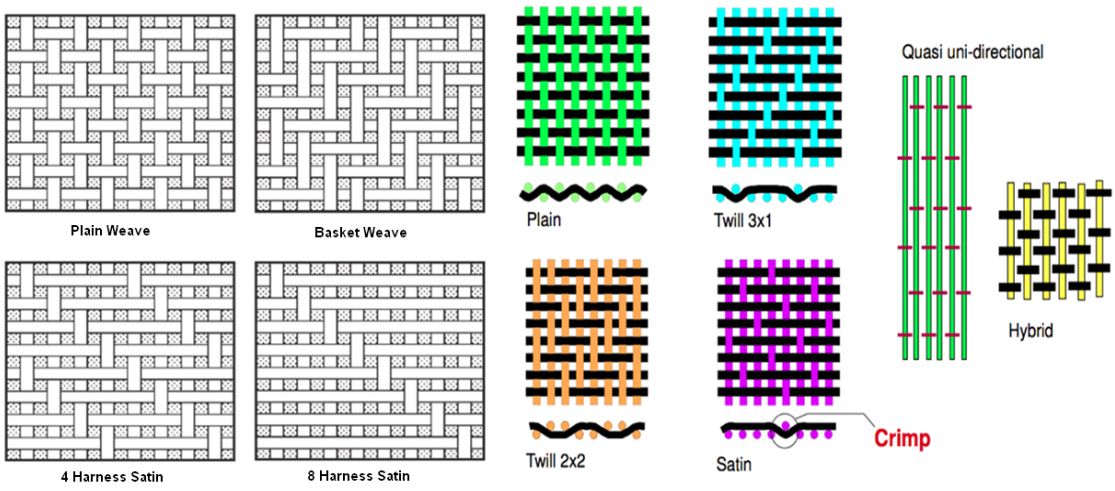

Figure 2-9: Different types of woven fabrics: hybrid and uni-directional [16,23].

d. Tri-axial weave:

The tri-axial weave is made of three sets of yarns separated by a 60° angles. This type of fabric has excellent tear, shear and bursting resistance. It is used for sailcloth, balloon fabric and laminated reinforced structures.

3. Mats:

The mat is normally made of relatively short fibers and is used in noncritical applications. However, mats can also be made using continuous fibers. The continuous mat is produced by swirling strands of continuous fibers onto a belt, spraying a binder over them, and drying the binder; this is then called swirl mat.

4. Braids:

The procedure of making braid fabrics is somehow similarly to that of weave fabrics; the difference is that warp and weft yarns are replaced in braids by two sets of yarn spools that turn in opposite directions around a mandrel. The most common types of braided structures are Diamond braids, Regular braids, Hercules braids, and Tri-axial braids. They are somehow equivalent to plain weaves, 2/2 twill, 3/3 twill, and tri-axial weaves.

5. Hydrides:

Reinforcement schemes that combine two or more types of reinforcements are called hybrids such as carbon/aramid. The advantages of hybrids are that in some weaves and braids, the best properties of each of the types of reinforcements can be utilized.

2.3.5 Carbon fibers properties

Carbon fibers are high strength materials and offer the highest specific modulus and highest specific strength of all reinforcing fibers [16,23]. Table 2.4 [17] shows different precursors of carbon fiber and their axial tensile properties and illustrates that the strength of carbon fibers depends on the production process.

Table 2.4: Axial tensile properties of carbon fibers [17].

Precursor	Tensile Strength (GPa)	Tensile Modulus (GPa)	Elongation at break (%)
PAN	2.5-7.0	250-400	0.6-2.5
Mesophase Pitch	1.5-3.5	200-800	0.3-0.9
Rayon	≈ 1.0	≈ 50	≈ 2.5

Carbon fibers do not suffer from stress corrosion or stress rupture at high temperature as other fibers do. They have found suitable applications in composites requiring exceptional strength, high stiffness, low weight and outstanding fatigue characteristics. Similarly, carbon fibers are good for high temperature, chemical inertness and high damping properties. They are also good conductors with electrical conductivity values in the order of 104 S/cm. This conductivity is assumed to arise from the natural conductivity of graphite and the orientation of the graphene rings, which are parallel to the axis of the fiber. Pitch fibers have a better electrical conductivity than PAN based fibers. Moreover, Carbon fibers have good thermal conductivity,

and low linear coefficients of thermal expansion. Some kinds of carbon fibers have high compressive strength (i.e. PAN based) as will be discussed below [17]. PAN based carbon fibers have higher tensile and compressive strength than pitch based carbon fibers because PAN based fibers have a particle-like structure and smaller crystals as compared to the sheet-like structure and larger crystals in pitch based fibers. The cross-sectional structure of carbon fibers also plays an important role in determining compressive properties of carbon fibers. The differences in cross-sectional structure result from preparation conditions of the procedure [17]. It has been found that the compressive strength increases with decrease in crystal size, density, and with increase in inter-planar spacing and void content. On the other hand, the compressive strength decreases with increase in modulus of elasticity for both pitch and PAN based fibers [16].

2.4 Fiber reinforcement of aluminium matrix composites

The main objective of reinforcing aluminium and its alloys using carbon fibers is to enhance strength and stiffness while maintaining primary properties of aluminium which are light weight, good thermal and electrical conductivity [17]. Other properties are also improved in the final composites such as service temperature, wear resistance, elastic modulus, coefficient of thermal expansion, creep and fatigue properties. The final properties of the composite are influenced by fiber type, fiber content, fiber orientation, fiber length, fiber distribution, and fiber/matrix bond [17].

2.4.1 Fiber content

The fiber content or fiber volume fraction plays an important role in the final properties of the composites as expressed in the rule of mixture Equation (2.1):

$$P_c = P_m V_m + P_r V_r \tag{2.1}$$

Where P = property; V = volume fraction; and subscripts m and r indicate the matrix and the reinforcement respectively [17]. The strength of the composite increases nearly proportionally with carbon content as illustrated in Figure 2-10 [10,24,25].

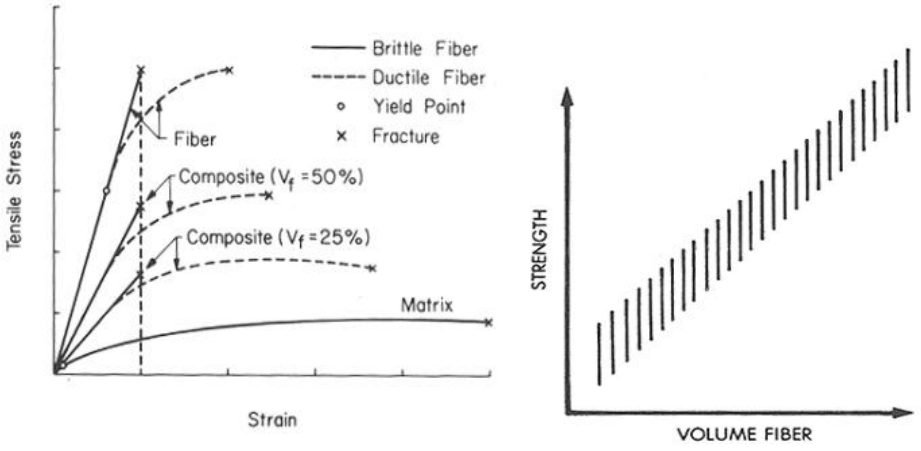

Figure 2-10: The effect of fiber content on the strength of composites [26,27].

2.4.2 Fiber orientation and distribution

Fiber orientation and distribution have great effects on the properties of composites. Figure 2-11 shows different types of fiber orientations in composites [26,27].

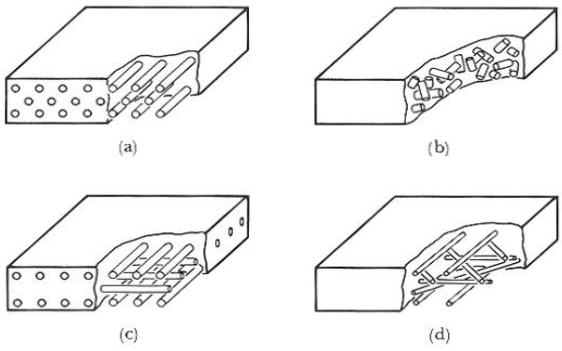

Figure 2-11: Different types of fiber orientation in composites: a) unidirectional; b) random; c) bidirectional; and d) multi-directional for different planes [26,27].

As seen in Figure 2-12, the composite behavior differs as the load is applied in different directions with respect to the fiber orientation. Unidirectional composites have the greatest strength of all composites with a load aligned with the fibers; in other directions their strength decreases considerably and depends on the matrix material. For the bidirectional composites, the ultimate strength is lower, but occurs in two directions. As the direction of the fibers becomes more statistically distributed throughout the composite, the ultimate strength decreases, but the properties are more uniform in all loading directions [24,28].

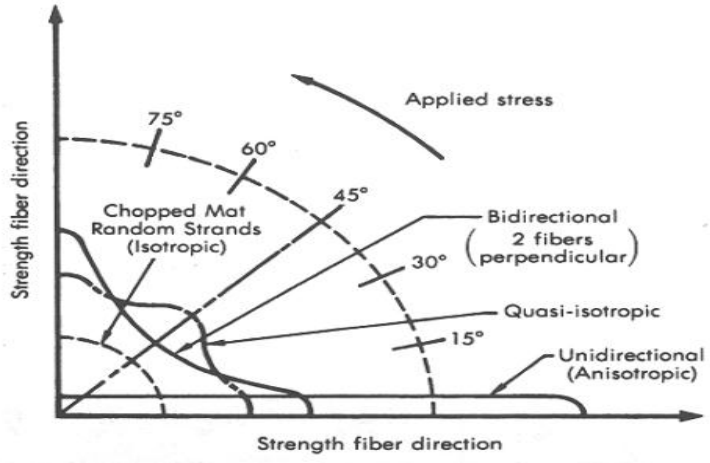

Figure 2-12: Dependence of composite properties on fiber and loading orientations [24,28].

The distribution of the fibers also has an effect on the final properties of the composite. The more uniformly the chopped fibers are distributed, the higher the strength of the composite is [24,28].

2.4.3 Fiber length

The fiber length is crucial for the effective strength and stiffness of the composite material. The critical fiber length l_c depends on the fiber diameter d, the fiber ultimate strength σ_f and the fiber/matrix bond strength or shear yield strength τ_c according to Equation (2.2):

$$l_c = \frac{\sigma_f d}{2\tau_c} \tag{2.2}$$

In most carbon fiber/matrix combinations, the critical fiber length is in the order of 1 mm, which ranges between 20 and 50 times the fiber diameter. Figure 2-13 a, b and c shows the stress distribution for a fiber reinforced composite that is subjected to a tensile stress equal to the fiber ultimate (tensile) strength when the fiber length is equal to the critical length, greater than the critical length, and less than the critical length respectively [29].

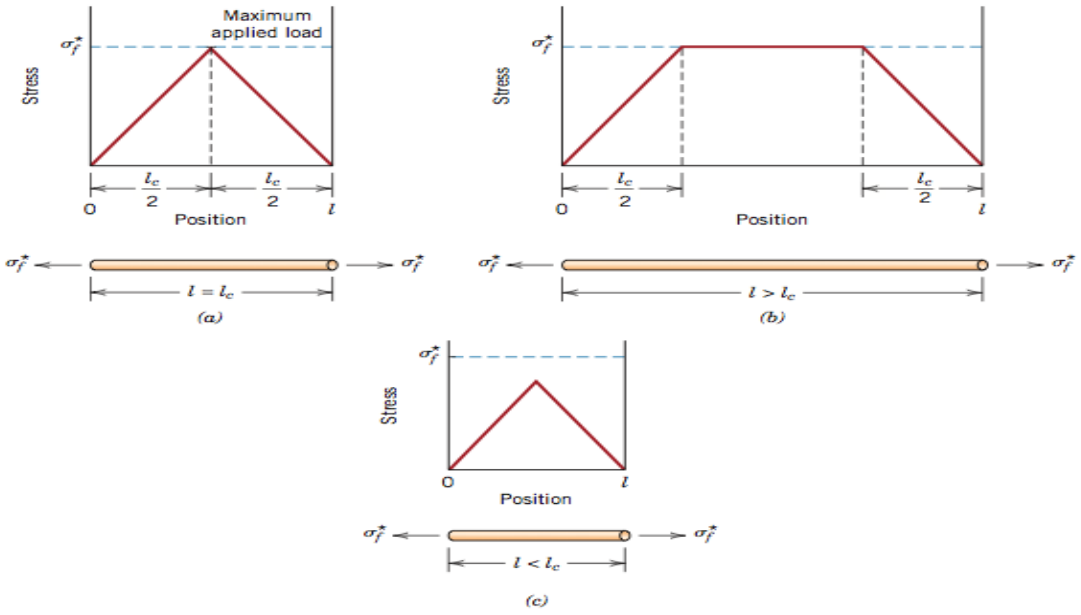

Figure 2-13: Stress profiles when the fiber length l: (a) is equal to the critical length lc; (b) is greater than the critical length; and (c) is less than the critical length for a fiber-reinforced composite that is subjected to a tensile stress equal to the fiber tensile strength σ_{f*} [9,29].

Thus, as the fiber length increases, the fiber reinforcement becomes more efficient. $l > 15\ l_c$ applies for continuous fiber. On the other hand, short or shopped (discontinues) fibers have lengths shorter than the critical length, in which case the matrix deforms around the fiber and there is no complete stress transfer from the matrix to the fibers, and the composite behaviour is dependent on the discontinues fiber distribution [9].

2.4.4 Fiber/matrix interface bond

The fiber/matrix bond plays an important role in the load transmission from the matrix to the fibers. It is essential that this bond is strong for the composite to develop the desired properties. Figure 2-14 shows different fiber configurations in a composite and the matrix deformation pattern around the reinforcement fibers. At too low bond strength, the fibers can slide within the matrix, and thus cannot carry any load, but rather can weaken the matrix due to the volume occupied by the ineffective fibers, potentially leading to composite failure.

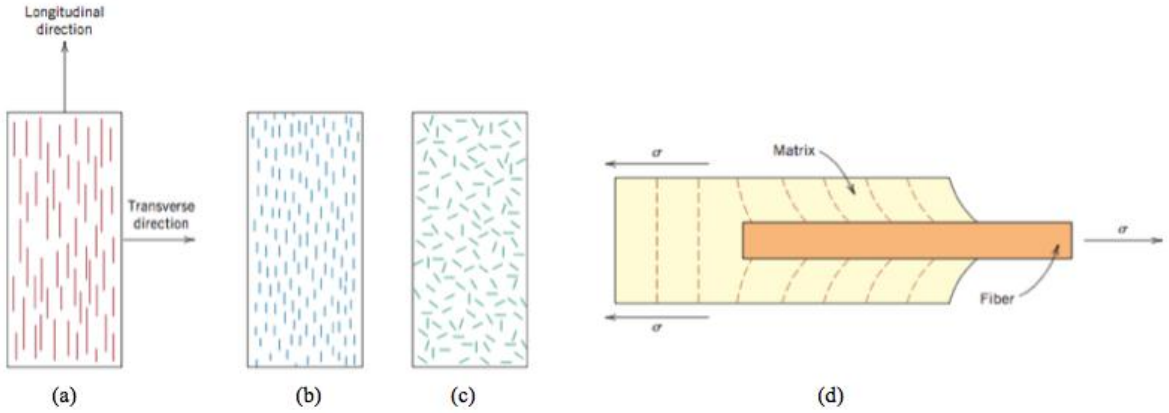

Figure 2-14: Schematic representations of: (a) continuous and aligned; (b) discontinuous and aligned; (c) discontinuous and randomly oriented fiber reinforced composites; (d) the deformation pattern in the matrix surrounding a fiber that is subjected to tensile load. The fiber/matrix bond influences the deformation pattern [9].

The fiber/matrix bond can be classified into three types:

Mechanical bond: This type of bond can be produced by different contractions, which could achieve a satisfactory bond provided an appropriate choice of materials is available. Mechanical bond includes interlocking effects due to wetting of the fibers or external bond agent. Wetting of the fibers can be achieved by subjecting the fibers to very high pressure produced within the liquid matrix during the squeeze casting process. However, this method has limitations because squeeze casting cannot be subjected to all types of composites. For this reason, another method

has been found to achieve mechanical bond by using external bond agents. External bond agents include copper, zinc or magnesium coating of fibers, but the results are often not fully satisfactory because of corrosion problems bond agents can pose at the interface [24,30].

Chemical diffusion bond: It is also called adhesion bond which involves some limited dissolution of one or both components into the other and can result in a good bond provided that defects such as voids are not produced at strategic places in the interface structure. During the liquid infiltration method (LIM) of aluminium matrix into carbon fibers, adhesion bond is determined by conflicting effects where carbon is dissolved in liquid aluminium and aluminium diffuses into the carbon fibers. After cooling, carbon atoms remain in the matrix, even if they are undetectable by TEM. The remaining carbon atoms in the matrix can create aluminium carbides by reaction with liquid aluminium [31,32].

Chemical reaction bond: It is usually formed by reaction products at the interface between the fiber and the matrix. Since such reaction products are likely to be brittle, their thickness is usually limited to below a critical thickness. In fact, above this critical thickness, cracks in the brittle interface phase may be sufficiently large to initiate fracture in the fiber itself or in the composite as a whole, while below the critical thickness the crack generally remains small and stable [32,36].

2.5 Manufacturing of metal matrix composite materials

Metal matrix composite materials are produced by either casting or powder metallurgy methods depending on the type of hardening particles and intended application conditions [11]. The most common metal matrices are aluminium, aluminium-lithium, magnesium, copper,

titanium alloy, and superalloy based. Hardening particle or fiber materials are usually graphite, carbon, oxides, carbides, boron, molybdenum and tungsten [33].

The current thesis focuses on aluminium based composites reinforced with carbon fibers. Most fiber reinforced aluminium based composites are manufactured by casting. Different casting methods are used depending on the nature of the aluminium alloys. Most commonly squeeze casting, liquid metallurgy (stir casting), or powder metallurgy are used [11,33].

2.5.1 Squeeze casting

Squeeze casting combines the advantages of traditional high-pressure die casting, gravity permanent mold die casting and common forging technology [11]. It was developed in the 1960s and involves the solidification of molten metal under high pressure to eliminate casting defects [25,33]. In contrast to standard casting methods, no gating system is used in squeeze casting and the liquid metal is pressed in tight contact with the die walls preventing air gap formation at the casting-die interface. Since pressure is applied, defects such as porosity and shrinkage are eliminated. In addition, the casting yield is practically 100% due to the absence of the gating system. Finally, the heat transfer rate is higher and finer grain castings featuring higher strength can be produced [12,25].

In standard squeeze casting, the liquid metal is injected into the interstices of short fiber usually called preform. The liquid metal remains pressurized while it solidifies. The pressure required for infiltration can be calculated based on the necessary meniscus. Correction can be made for the melt-fiber wetting. In most cases, fibers do not act as preferential crystal nucleation sites during melt solidification. The last liquid to freeze, which is usually solute-enriched, tends to be located around fibers. Figure 2-15 illustrates the layout of the squeeze infiltration

apparatus, and Figure 2-16 shows a flow diagram describing the squeeze casting infiltration process [25,33]. The casting operation consists of first preheating the die containing the preform typically to 300–400°C and melting a weighed charge of the alloy to be cast at a temperature typically between 150–250°C above its liquidus temperature. The molten metal is then poured into the die and the punch is driven into the die cavity at a constant ram speed of about 10 m/s to compress the charge [12,25]. In most cases, the optimum pressure is 20 to 30 MPa which prevents separation between the fibers and the matrix material resulting in a maximum strengthening effect [34]. The pressure is maintained during solidification and an additional 5–10 minutes further cooling period. The ram is then withdrawn and the composite ejected [12,25].

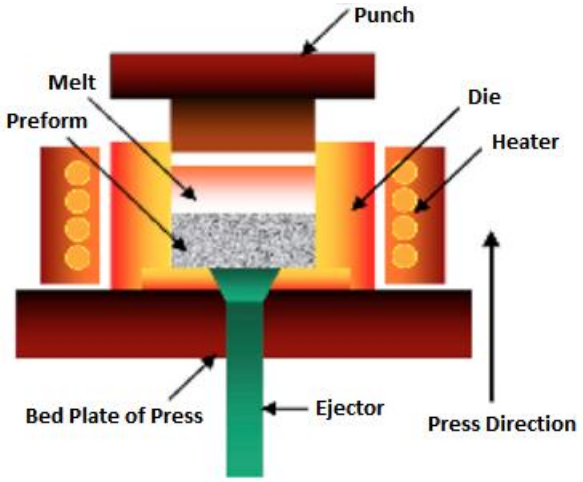

Figure 2-15: Diagram illustrating the layout of the squeeze infiltration apparatus [12,25].

The followings are the major process parameters during squeeze casting [12,25].

- molten metal temperature
- melt volume
- melt quality and quantity
- preform preheat temperature
- die design and preheat temperature
- applied squeeze pressure
- pressure application duration
- lubrication level

Common squeeze casting defects include:

- oxide inclusions
- porosity and voids
- blistering cold laps and cold shuts
- sticking of casting with die surface

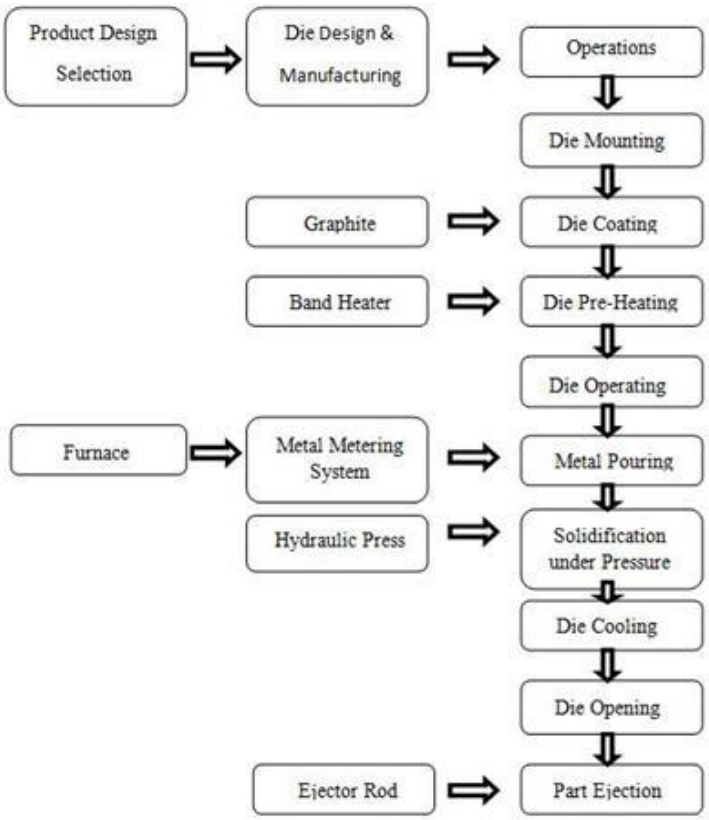

Figure 2-16: Flow diagram describing the squeeze casting infiltration process [40].

2.5.2 Stir casting

Molten metal mixing casting or "stir-casting", as named by Vogel [35], is the production of metallic materials by a shearing action induced by stirring. It involves melting a selected matrix material followed by the introduction of a reinforcing material into the melt and obtaining a suitable dispersion through stirring. This method of casting is an easy way for producing particle reinforced aluminium alloys [36,37].

This technique of casting metal matrix composites has more flexibility, is less expensive and is more applicable to large production quantity than other methods of casting [33]. Using this semi-solid metallurgy technique has several factors that must be considered. These factors are a uniform distribution (i.e. homogenous composition) of the reinforcement material; a high wettability between the two elements; less porosity in the cast metal matrix composite; and avoiding chemical reactions between the reinforcement material and the matrix alloy.

The stir casting process begins with the preparation of the raw matrix material. Then the matrix materials are placed in a container inside a furnace with a nitrogen environment. The container is heated above the melting point of the matrix material until melting is completed. The particles (i.e. reinforcements) are injected in an inert carrier gas into the melt with an injection gun, using reciprocating rods (impeller) to push the particles into the melt. Good distribution of the reinforcement material is achieved by using the vortex method that consists in stirring the melted matrix vigorously to form a vortex at the surface of the melt. At the side of the vortex, reinforcement material is introduced and then stirred continuously for a few minutes until the composite mix has cooled into a slurry and is then cast [37,38].

The most important variables during casting of metal matrix composites by stir casting include:

- Increasing stirring speed and stirring time leads to a more homogeneous distribution of the reinforcement into the metal matrix and to higher hardness of the composite [39].
- Good wetting between the particles and the matrix can be promoted by several methods: coating the particles with wettable metals; adding alloying elements to the molten matrix

alloy; treating the particles before adding them to the matrix, and ultrasonic irradiation of the melt [37].

- Pores in the composite can entrap gases during mixing, hydrogen evolution and shrinking during solidification. Porosity can be reduced by optimizing parameters such as holding time, stirring speed, size and position of the impeller. Also, casting in vacuum, degassing, casting under pressure, closing pores by compressing, extruding and rolling can be used to reduce porosity [37].

2.5.3 Powder metallurgy

Throughout the history of manufacturing, powder metallurgy (PM) technique has been used to manufacture a large variety of solid materials. It was initially used in India and Africa back in 1200 BC. It was established as a viable method for industrial production of high quality materials early in the 20^{th} century with the commercial success of self-lubricating bearings [14]. Powder metallurgy is a solid state process. In its simplest form, PM consists in producing, blending and compacting powders to a solid compact called green, followed by heat treatment also called sintering of the green. Figure 2-17 shows the classic powder metallurgy process.

The advantages of using PM for manufacturing MMCs include [14,40]:

- Interfacial reactions such as reactions between the matrix and the reinforcement can be limited or eliminated due to substantially lower process temperatures compared to other methods.
- Improved homogeneity of the reinforcement distribution in the matrix due to the solid-state nature of the process with reduced tendency for phase segregation. This

composite uniformity improves both the structural properties (i.e. porosity, toughness and stiffness) and their reproducibility.

- Materials that cannot be manufactured using melting processes such as casting due to extremely high melting points of the constituents or strong differences in melting points and densities can be better produced by PM.

The disadvantages of using PM include:

- Potentially more expensive than conventional processes such as casting for simple geometries and alloys.
- Generally higher equipment costs.
- Handling of powders can be hazardous.

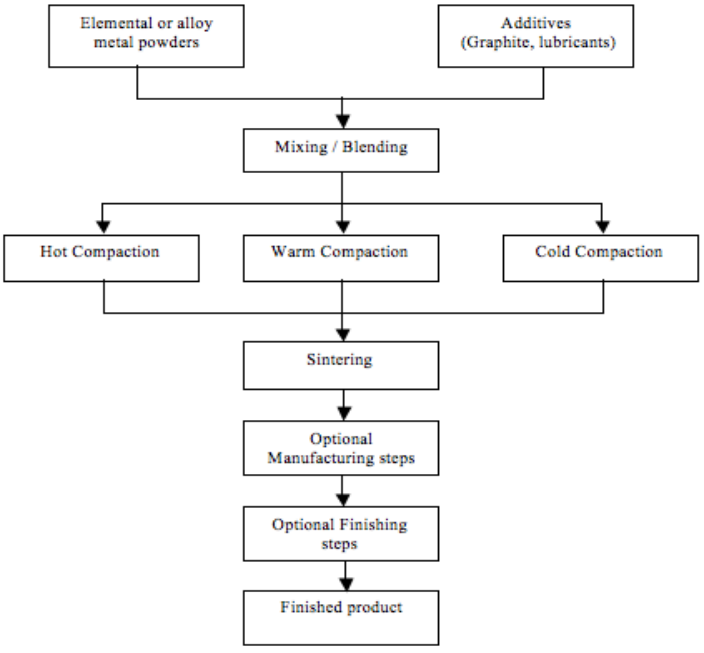

Figure 2-17: Summary of the classic PM process [11].

2.6 Properties of aluminium matrix composites

Table 2.5: Summary of advantages and disadvantages of aluminium matrix composites compared to competing materials [1,10].

Advantage	Disadvantage
Compared to un-reinforced aluminium	
➢ Higher specific strength ➢ Higher specific stiffness ➢ Improved high temperature creep resistance ➢ Improved wear resistance	➢ Lower toughness and ductility ➢ More complicated and expensive ➢ Complicated production method
Compared to polymer matrix composites	
➢ Higher transverse strength ➢ Higher toughness ➢ Better damage tolerance ➢ Improved environmental resistance ➢ Higher thermal and electrical conductivity ➢ Higher temperature capability	➢ Less developed technology ➢ Smaller data base of properties ➢ Higher cost
Compared to ceramic matrix composites	
➢ Higher toughness and ductility ➢ Ease of fabrication ➢ Lower cost	➢ Inferior high temperature capability

Aluminium matrix composites are used in advanced applications because they combine high strength, low density, durability, machinability, availability and cost effectiveness; thus they have substantial advantages compared to competing materials [1,10]. Table 2.5 shows a comparison of the advantages and disadvantages between aluminium matrix composites and some competing materials.

The main purpose of making composites is to enhance the desirable properties for use in a wide range of applications. The desired properties include low density; high stiffness; high strength; thermal and electrical conductivity; fatigue, creep and wear resistance as discussed in the following sections [41].

2.6.1 Density

One of the important properties that encouraged researchers to produce aluminium matrix composite materials is lightweight that can be controlled through the density. Aluminium matrix composite density can be estimated using the rule of mixture Equation (2.3):

$$\rho_c = \rho_m V_m + \rho_r V_r \tag{2.3}$$

Thus, the density and the volume fraction of both reinforcement and matrix determine the density of the final composite [42].

2.6.2 Stiffness

The stiffness of the composite can be described through the elastic modulus, which is sub-divided into two models. The first model follows the linear upper bound reinforcement that can be defined by the simple rule of mixture as shown in Equation (2.4). This expression is applied for continuous fiber [23,41].

$$E_C = E_m V_m + E_r V_r \tag{2.4}$$

The second model is valid for non-linear bound and for non-continuous fiber. This expression is more complex as seen in Equation (2.5) [23,41].

$$E_c = \frac{E_m V_m + E_r (V_r + 1)}{E_r V_m + E_m (V_r + 1)} \tag{2.5}$$

It is clear from the above considerations that the addition of either short fibers or continuous fibers with high stiffness can increase the stiffness of the aluminium matrix composites substantially.

2.6.3 Strength

The material strength is difficult to predict accurately by simple mathematical expressions and is determined by the matrix alloy, the reinforcement and the processing. Two major contributions to the yield stress are matrix strengthening effects and residual thermal stresses due to differential contractions of reinforcement and matrix. Figure 2-18 shows the stress-strain curve behavior for unreinforced aluminium matrix and carbon fiber reinforced aluminium [43].

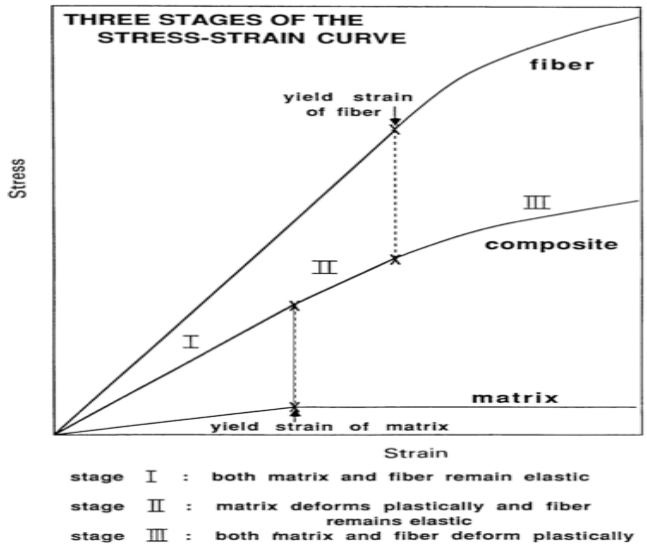

Figure 2-18: The stress-strain curve behavior for unreinforced aluminium matrix, carbon fiber, and carbon fiber reinforced aluminium matrix composite [43].

For continuous uniaxial fiber composites, the rule of mixtures can be used to predict the fracture strength (σ_c^F) of the composite in axial tensile conditions as can be seen in Equation (2.6):

$$\sigma_c^F = \sigma_m V_m + \sigma_r V_r \tag{2.6}$$

Where σ_i is the tensile strength and V_i is the volume fraction of matrix (i = m) and fiber reinforcement (i = r). However, composite properties mostly fall below the theoretically expected values, due to misalignment of the fibers and inhomogeneity in fiber distribution. The ratio of

transverse to longitudinal strength is for most aluminium based composites in the range of 0.12 to 0.33 [43]. For multidirectional loading of the composite, the use of composites with different fiber orientations is recommended and the strength can vary with orientation.

The fracture strength of discontinuous fiber composites depends on type, aspect ratio, volume fraction and distribution of the reinforcement, on the matrix alloy and its heat-treatment conditions, as well as on the fiber/matrix bond [10,43].

For aligned fibers, a modified rule of mixture provide a better prediction of the longitudinal strength as can be seen in Equation (2.7):

$$\sigma_c{}^F = \sigma_r{}^F \left(l - \frac{l_c}{2l}\right) V_r + \sigma_m V_m \tag{2.7}$$

Where σ_m is the stress carried by the matrix at failure, l is half the length of a fiber, l_c is the minimum or critical fiber length capable of carrying the fracture stress of the fibers [43].

2.6.4 Thermal expansion, thermal and electrical conductivity

The thermal expansion coefficient of aluminium matrix composites reinforced with carbon fiber is much lower compared to that of polymer matrix composites, meaning that the aluminium matrix composites expands much less when subjected to higher temperature. The coefficient of thermal expansion (α_c) of the composite can be approximated by the following rule of mixture [10,43] ;

$$\alpha_c = \frac{\alpha_m V_m K_m + \alpha_r V_r K_r}{\alpha_m V_m + \alpha_r V_r} \tag{2.8}$$

Where K_i is the thermal conductivity; α_i is the thermal expansion; and V_i is the volume fraction of matrix (i = m) and fiber reinforcement (i = r).

Using a sufficiently high volume fraction of reinforcement, the coefficient of thermal expansion of the Al-based composite can be reduced to the level of steel. With carbon fibers,

which have a negative coefficient of thermal expansion, aluminium composites with a coefficient of thermal expansion even close to zero can be produced.

The ability of aluminium to conduct electrical current is higher than that of carbon fiber. Therefore, Al-composites with high carbon fiber volume fraction show low electrical conductivity. The electrical conductivity of composites can also be described by the rule of mixture. In addition, the electrical conductivity of the composites is influenced by temperature during use. As the application temperature for aluminium matrix composites increases, the ability of the current to pass through the composites decreases [42].

2.6.5 Fatigue

The fatigue properties of aluminium composites are usually better than those of unreinforced equivalent alloys particularly in the high cycle fatigue range [42]. However, the low cycle fatigue properties of composites can be somewhat worse than those of unreinforced alloys because of the lower ductility in composites due to carbon fiber reinforcement. For continuous fiber composites, uniaxially reinforced alloys usually possess excellent fatigue properties when oriented parallel to the major fiber axis. Values of the fatigue/tensile strength ratio (at 10^7 cycles) between 0.55 and 0.8 are not unusual [42]. For discontinuously reinforced composites, where the reinforcement produces an increase in tensile strength, it is usual that the fatigue strength will also be improved, particularly under low cycle fatigue conditions. However, the effect of particulate reinforcement depends upon particle size and volume fraction. Also, inhomogeneities and particle clusters have a negative influence on the fatigue strength [42].

2.6.6 Creep

Creep is the tendency of a solid material to slowly move or deform permanently with time under the influence of stress [10]. It occurs as a result of long-term exposure to high temperature, generally under stresses below the yield strength of the material. Mathematically, creep can be expressed through the steady state creep Equation (2.9) [10]:

$$\dot{\varepsilon} = A\sigma^n \exp\left(\frac{-Q}{RT}\right) \tag{2.9}$$

Where $\dot{\varepsilon}$ is the creep rate; A a constant; σ the creep stress; n the stress exponent; Q the activation energy; R the gas constant; and T the absolute temperature.

At low stress and strain rate, n is high and increases with decreasing stress. At high stresses and strain rate, n tends towards a constant value. It has been proven that the creep rate decreases with increases in reinforcement content and threshold creep stress [42].

2.6.7 Wear resistance

The wear of AMCs depends on the particular wear conditions, but there are many circumstances where Al-based composites have excellent wear resistance. It has been found that the coefficient of friction and the wear rate of Al-based composites drop to their lowest values at about 100°C and thereafter increase with increasing temperature. Also, the coefficient of friction and the wear rate decrease with increasing carbon fiber volume fraction [44].

3 METHODOLOGY

3.1 Materials description

In general, a composite material contains at least two main elements, which are the matrix and the reinforcement. Other elements may be added based on the composition and the intended application. In this work, aluminium is used as matrix and the reinforcement consists of fabrics made of woven carbon fiber filaments.

3.1.1 Aluminium

Wrought aluminium 1235 is selected as matrix material in most of the samples and 6061 aluminium alloy mixed with 1235 aluminium alloy in the rest of them. Aluminium 1235-H19 foil is chosen due to its desirable properties such as light weight, high corrosion resistance, easy fabrication, low strength, workability, conductivity and non-heat-treatable nature. Compositions as well as physical, mechanical, electrical and thermal properties of the 1235 foil are tabulated in Table 3.1and Table 3.2 respectively.

Table 3.1: Element percentages for aluminium 1235-H19 foil.

Elements	Percentages
Aluminium, Al	>= 99.35 %
Copper, Cu	<= 0.050 %
Magnesium, Mg	<= 0.050 %
Manganese, Mn	<= 0.050 %
Si+Fe	<= 0.65 %
Titanium, Ti	<= 0.060 %
Vanadium, V	<= 0.050 %
Zinc, Zn	<= 0.10 %
Other, each	<= 0.030 %

Table 3.2: Physical, mechanical, electrical and thermal properties for Aluminium 1235-H19 foil.

Physical Properties	**Metric**	**Comments**
Density	2.705 g/cc	
Mechanical Properties	**Metric**	**Comments**
Brinell hardness	45	500 kg load with 10 mm ball
Ultimate tensile strength	165 MPa	
Yield tensile strength	145 MPa	
Elongation at break	2.50 %	Foil
Modulus of elasticity	69.0 GPa	Estimated from trends in similar Al alloys
Poissons ratio	0.330	Estimated from similar Al alloys
Shear modulus	26.0 GPa	Calculated value
Shear yield strength	100 MPa	
Electrical Properties	**Metric**	**Comments**
Electrical resistivity	3.10^{-6} ohm-cm	
Thermal Properties	**Metric**	**Comments**
Heat of fusion	390 J/g	@Temperature 20.0 -100°C
Linear coefficient of thermal expansion	23.6 μm/m-°C	Estimated from trends in similar Al alloys @ Temperature 20.0 -100°C
Specific heat capacity	0.900 J/g-°C	
Thermal conductivity	225 W/m-K	
Melting point	645 - 655 °C	
Solidus	645 °C	
Liquidus	655 °C	

3.1.2 Carbon fiber fabric AS4 Hexcel

Carbon fiber AS4 Hexcel is continuous 3,000 (3K) filament count tows. This fiber has been surface treated and sized to improve its interlaminar shear properties, handling characteristics, and structural properties. AS4 Hexcel continuous fiber was received as plain weave fabric as shown in Figure 3-1. AS4 Hexcel is made from high grade PAN based fiber and

it is suitable for high strength and strain applications. Physical, mechanical, electrical and thermal properties, and carbon percentages for AS4 Hexcel, continuous 3K are tabulated in Table 3.3.

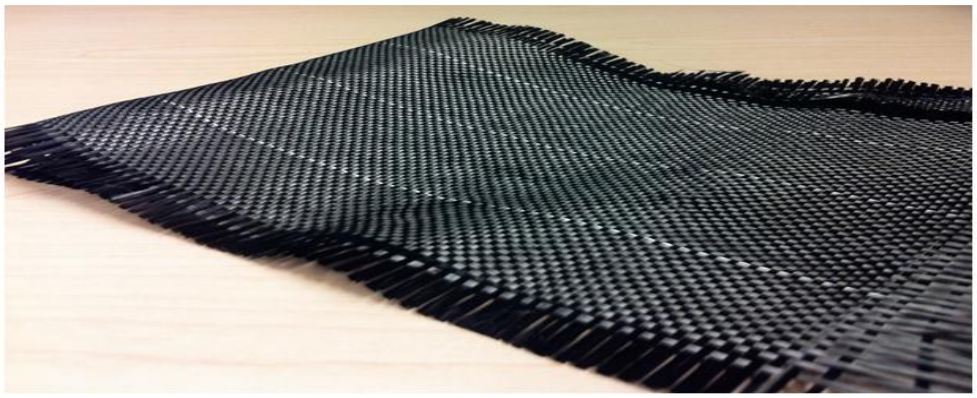

Figure 3-1: AS4 Hexcel plain weave carbon fiber fabric.

Table 3.1: Physical, mechanical, electrical, thermal properties, and carbon percentage for AS4 Hexcel, continuous 3K.

Properties	**Metric**
Tensile strength	4433 MPa
Tensile modulus	231 GPa
Ultimate elongation at failure	1.8 %
Density	1.79 g/cm^3
Weight/length	0.210 g/m
Approximate yield	4.76 m/g
Tow cross-section area	0.12 mm^2
Filament diameter	7.1 microns
Carbon content	94.00 %
Specific heat	0.27 Cal/g-°C
Electrical resistivity	1.7*10^{-3} Ohm-cm
Coefficient of thermal expansion	0.63 ppm/°C
Thermal conductivity	6.83 W/m-°K

3.2 Manufacturing process

3.2.1 Features of squeeze casting

Different aspects have been considered while designing the squeeze casting process such as high temperature and pressure application conditions. Stainless steel 304 is selected to make the components for the squeeze casting equipment due to its high yield strength, high melting temperature and high oxidation resistance. Although the yield strength of stainless steel 304 degrades at high temperature, it does not collapse at the temperature required in this application [45].

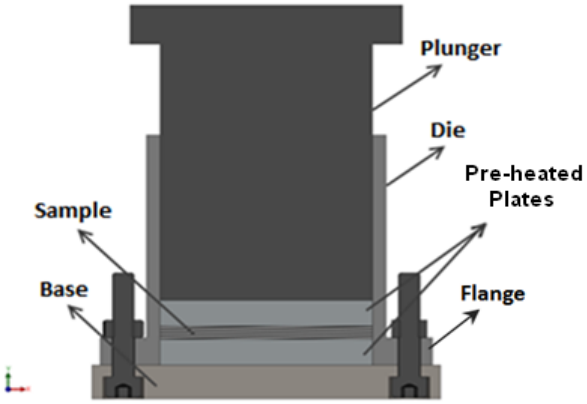

Figure 3-2: Squeeze casting setup.

Initially, the squeeze casting setup contained three simply removable parts, which are plunger, die, and base as shown in Figure 3-2. The die is designed to be cylindrical in order to achieve best sealing and uniform circumferential pressure. It has a diameter of 78 mm and 4 mm wall thickness and is welded to a flange of 122 mm diameter and 10.5 mm wall thickness. The plunger is a piston fit to the die and is designed to be longer than the die depth in order to also be used as sample ejector to easily release samples after squeezing. The base thickness is 13 mm and both faces are flat in order to prevent plastic deformation during squeeze casting. Joining the

base with the die flange is done using 18-8 stainless steel socket head cap screws and 18-8 stainless steel hex nuts.

Some modifications of the squeeze casting setup are introduced later during investigations due to some observed manufacturing defects. Two 1 cm thick stainless steel flat plates are added one between sample and punch and the other between sample and die base. The plates are pre-heated with the samples in order to reduce heat losses and rapid temperature drop at the sample contact surfaces during squeezing. The plates are piston fit to the die and help maintain the required temperature before and during squeezing.

3.2.2 Sample preparation

Firstly, aluminium foils are received from the supplier as $1m^2$ square sheet with 0.32 mm wall thickness. Each sheet is cut to small square pieces. Scriber and reference piece are used to draw the final shape that represents the die fit diameter for both foils and plates as shown in Figure 3-3. Also, a special shear machine is used to cut the edges of the foil. Aluminium plates are also received as square pieces of 2 mm thickness. A band saw is used to cut the edges of these plates.

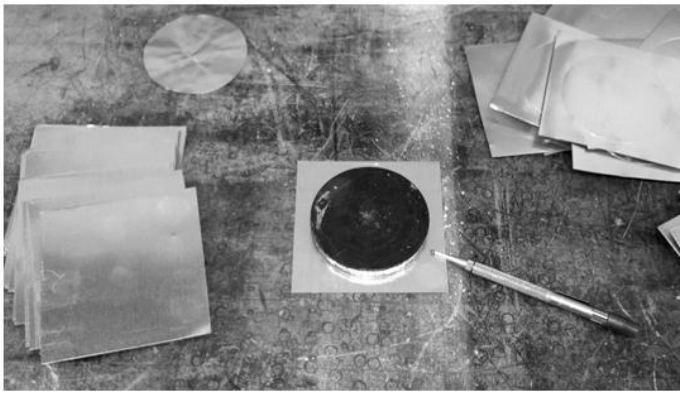

Figure 3-3: Scriber and reference piece used to draw the final shape of Al foils and plates.

Both aluminium foils and plates are combined together in array sequence and fixed using two pieces of wood to prevent the foils from bending while they are machined on the lathe. The carbon fiber fabric is first cut using scissors to a square shape. The square preform is then clammed and pressed between two aluminium plates and cut to the die shape (see Figure 3-4). This method is used to prevent the bundles from movements that may change the plain weave configuration.

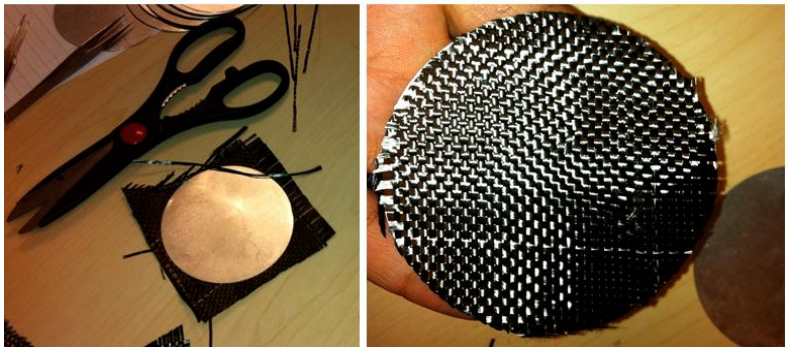

Figure 3-4: Method for preparing AS4 Hexcel preforms.

Other preparation processes are done on the fabric due to the experiment requirements. To reduce the carbon fiber density, tweezers are used to remove alternate yarns while keeping the same configuration of the plain weave as show in Figure 3-5. This process is easily done when the plain weave is still in square shape, before it is cut into the die circular shape as described above and shown in Figure 3-5. The final sample assembly and configuration in the die is shown in Figure 3-6.

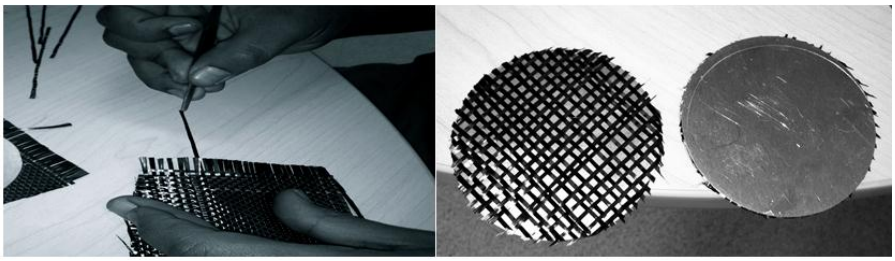

Figure 3-5: Low density fiber fabric achieved by removing alternate fibers.

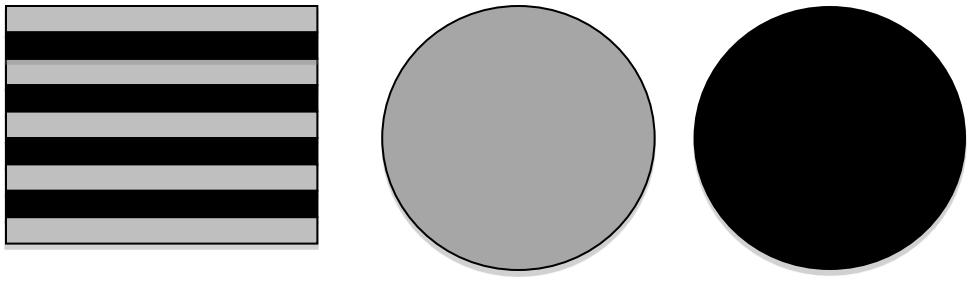

(a) (b) (c)

Figure 3-6: (a) Configuration of aluminium foils/carbon fiber fabrics in the squeeze casting die; (b) top view of aluminium foil; (c) top view of carbon fiber fabric.

3.2.3 Squeeze casting process

Squeeze casting combines the advantages of traditional high-pressure die casting, gravity permanent mold die casting and common forging technology [11].

Samples are placed in the die and heated using a LINDBERG conventional furnace to 850°C. The heating time from room temperature to 850°C is about an hour. Then die and sample are maintained at 850°C for 30-40 min in the furnace in order to homogenise the temperature distribution and decrease the viscosity of aluminium. The die is then placed in the squeeze equipment consisting of a hydraulic presser and a load cell. The plunger is then inserted into the die from the top and the pressure is applied. The squeezing process lasts 5 to 10 minutes during which appropriate further downwards plunger displacement is forced in order to approximately maintain constant pressure while liquid aluminium infiltrates the fibers and the composite solidifies, cools and shrinks. The squeeze pressure is approximately 20 MPa. Finally, the ram is withdrawn and the screws joining the base with the die are released. The composite specimen is then ejected by further pressing the plunger through the now baseless die cavity until the sample

is completely released. Figure 3-7 shows the equipment setup for the squeeze casting experiment.

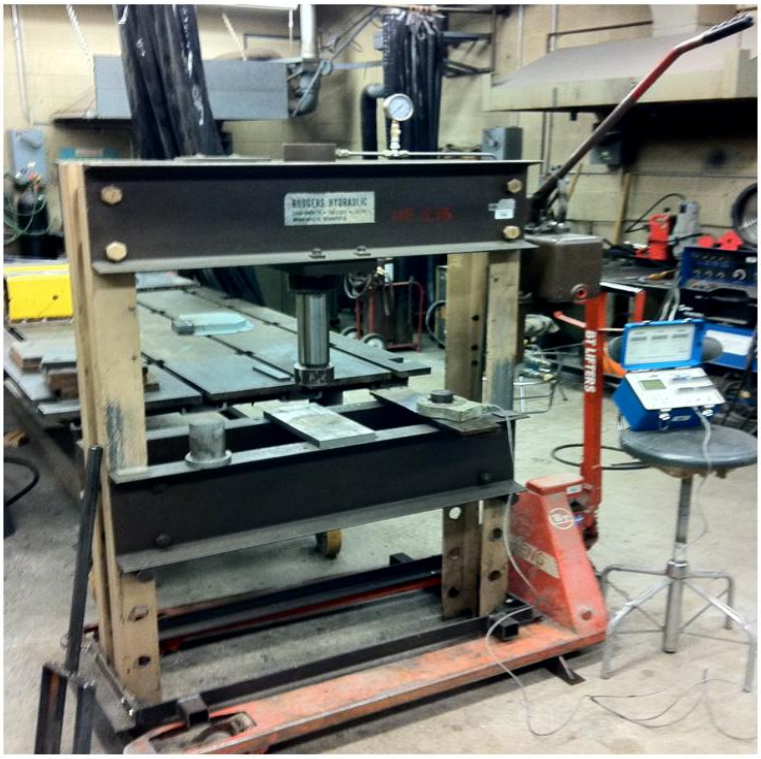

Figure 3-7: Equipment setup for squeeze casting.

3.3 Mechanical testing

3.3.1 Impact testing

The resistance of composite beam samples to breakage is determined using mini Charpy impact test as shown in Figure 3-8. Impact samples are beams of rectangular cross-section of width b (9.6 mm), thickness d (3.49-4.52 mm), and length l (55 mm). For the sake of simplicity, no notch is cut in the impact sample, which deviates from standard practice. The speed of the pendulum at the impact even is determined from the machine to be 3.46 m/sec. The test is performed at room temperature. Figure 3-9 shows the sample in the test fixture of the mini impact tester. As the samples have identical width but different thicknesses, the fracture energy

absorbed at impact is divided by the respective sample thicknesses resulting in specific values per unit thickness. The mini Charpy impact test provides a qualitative assessment of the energy needed to fracture the composite. Also, ductility and toughness of the composite samples are qualitatively assessed, and analysing the fracture surfaces gives an estimate of the failure mode, the percentage of ductile and brittle fracture [46].

Figure 3-8: Mini Charpy impact test equipment.

Figure 3-9: Specimen in test fixture of the mini impact tester.

The assessment is done visually for each sample. The fraction of brittle failure is considered to be the proportion of the sample cross-section that fractures during impact test,

while the fraction of ductile failure is considered to be the remaining portion of the sample cross-section that fails by delamination or by any other non-brittle mechanism.

3.3.2 Hardness testing

Hardness tests are performed at two scales: macro and micro. At the macro scale, Rockwell hardness tests are performed at room temperature with 150 kg indentation load as shown in Figure 3-10 and 3-11.

Figure 3-10: Rockwell tester used for determining macro hardness.

Although the tests proved to be off-scale leading to too deep indentations, the load is not reduced since the deep indentation meant better bulk testing of the laminate composites instead of merely testing the outer layers of the composite samples. The specimens are polished before testing using different sand paper scales to remove the oxide layers as well as to make the specimen surface flat and smooth. An optical microscope is used to measure the indentation diameter as illustrated in Figure 3-12. This test is done at least ten times for each specimen to cover some statistical variations. Mean average values and standard deviations are determined.

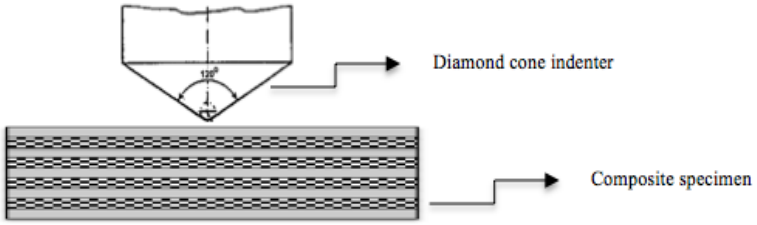

Figure 3-11: Cross-section of the Rockwell indenter cone and composite laminate.

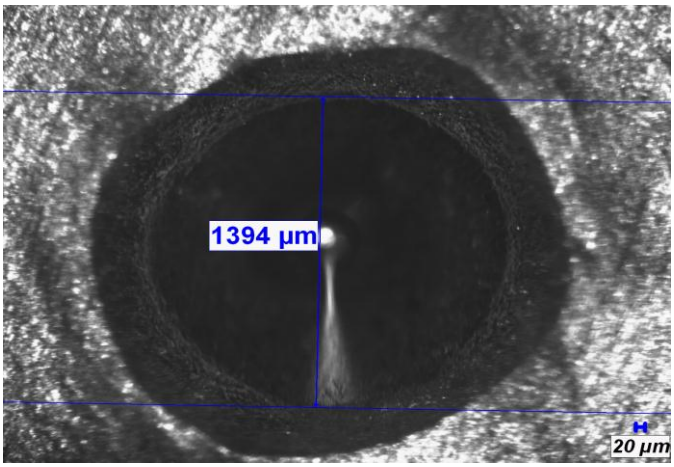

Figure 3-12: Indentation diameter measurement using optical microscopy.

At micro scale, Vickers hardness tests are used to investigate bonding and potential mix phase formation at carbon fiber/aluminium matrix interfaces. These investigations are done using a STRUERS DURAMIN A/S DK-2750 micro hardness testing machine equipped with an optical objective for direct measurement of indentation diagonals and hardness calculation as shown in Figure 3-13 and Figure 3-14. The HV number represents the Vickers hardness that is determined by the ratio *F/A* where *F* is the force applied and *A* is the surface area of the resulting indentation. The formula that the machine uses to calculate HV numbers is in Equation (3.1) and the results are reported as xxHV$_{YY}$, where xx is the reading result and yy is the load applied.

$$HV = \frac{2F\ sin\left(\frac{136^{\circ}}{2}\right)}{d^2} \tag{3.1}$$

Where F is load and d is arithmetic mean of the two indentation diagonals d_1 and d_2 as can be seen in Figure 3-14. An indentation load of 300 g (Hv0.3) and a holding time of 10 seconds are used.

Figure 3-13: STRUERS DURAMIN A/S DK-2750 micro hardness testing machine.

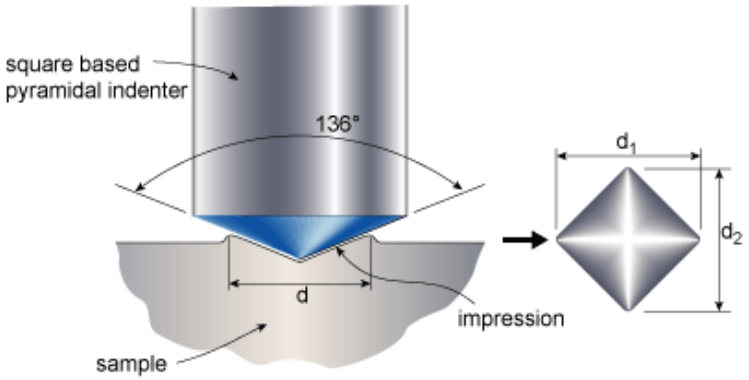

Figure 3-14: Sample indentation during Vickers hardness testing and illustration of the two indentation diagonals d_1 and d_2.

Mean value, standard deviation and coefficient of variation are calculated using Equations 3.2, 3.3 and 3.4 respectively.

$$\bar{x} = \frac{\sum_{i=0}^{n} x_i}{n} \tag{3.2}$$

$$S = \left[\frac{\sum_{i=0}^{n}(x_i - \bar{x})^2}{n-1}\right]^{(1/2)} \tag{3.3}$$

$$c_v = \frac{S}{\bar{x}} \tag{3.4}$$

3.3.3 Three point bend test

Three point bend tests are used to assess the short-beam strength of the composite samples. The composite specimens are beam of rectangular cross-section of width b (12 mm), thickness d (3.49-4.52 mm), and length l (40 mm). The specimen is installed on a two-roller support with a span length L (32 mm) as shown in Figure 3-15. An Instron universal test frame is used to apply the load (see Figure 3-16). The cross-head displacement speed is 10 mm/min and the deflection is measured up to 10 mm.

In theory, three point bending is basically considered as quasi-static bending of beam so the Euler-Bernoulli bending approach is valid. The Euler-Bernoulli equation for the quasi-static bending of slender, isotropic, homogeneous beams of constant cross-section under an applied traverse load q(x) is written as [47]:

$$EI\frac{d^4w(x)}{dx^4} = q(x) \tag{3.5}$$

Where E is the young's modulus, I is the area moment of inertia of the cross-section, and w(x) is the deflection of the neutral axis of the beam. Using this test method, bending flexural stress and bending flexural (transverse) modulus for composite specimens have been investigated. The classic formula for determining the bending (flexural) stress in a beam under simple bending has been used as:

$$\sigma_f = \frac{M_y}{I_x} \tag{3.6}$$

Where σ_f is the bending stress; M is the moment about the neutral axis; y is the perpendicular distance to the neutral axis; I_x is the second moment of area about the neutral axis

x. The flexural modulus can be obtained from Hooke's law as seen in Equation (3.7).

$$E_f = \frac{\sigma_f}{\varepsilon_f} \tag{3.7}$$

Where E_f is the flexural modulus; ε_f is the flexural strain; and σ_f is the flexural stress.

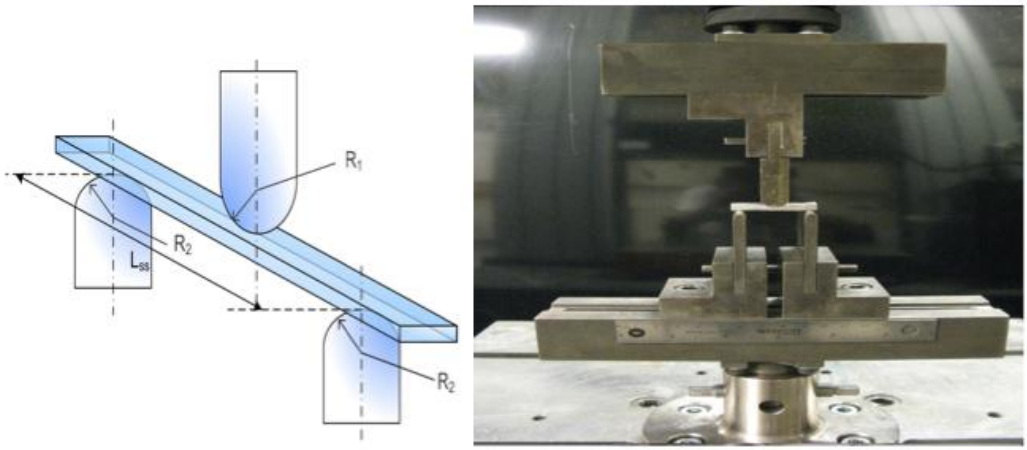

Figure 3-15: Test setup and supports for the bend tests.

Figure 3-16: Computer controlled Instron universal testing machine used for the bend tests.

Flexural stress, strain and modules are calculated using Equations 3.8, 3.9 and 3.10 respectively.

$$\sigma_f = \frac{3PL}{2b\,d^2} \tag{3.8}$$

$$\varepsilon_f = \frac{6Dd}{L^2} \tag{3.9}$$

$$E_f = \frac{L^3 m}{4b\,d^3} \tag{3.10}$$

Where P is the load at a given point on the load-deflection curve (N), *D* is the maximum deflection of the center of the beam (mm), and m is the slope of the initial elastic section of the load-deflection curve. Bend tests served only the purpose of relative comparison between different composite sample types; no statistical variations or standard deviations could be calculated due to the very limited number of test samples.

3.4 Microscopy

Metallographic samples are prepared for all sample types for the states before and after mechanical testing. The preparation included cutting samples using a digitally controlled STRUERS Secotom-10 with a spindle speed of 2000 rpm and silicon carbide cutting plates. The specimens are then mounted under 20 kN load at 150ºC for 12 min in epoxy resin using a STRUERS LaboPress-3.set machine. Grinding and polishing are carried out using a STRUERS Tegrapol-31 machine. The polishing parameters are 2000-rpm disc speed, single sample and manual preparation. Grinding and polishing are done according to the following steps:

- Grinding Piano 120 for 1 minute
- Allegro 9 micrometer, Diamond for 3 minutes
- Dac (blue color), 3 micrometer, Diamond for 3 minutes

- Nap, 1 micrometer, Diamond
- Chem, 0.04 micrometre OPS SIC

Each grinding and polishing step is followed by thorough cleaning to remove loose particles that may cause scratches during subsequent finer steps. Cleaning is done using water and ethanol ultrasonic bath. In addition, all optical microscopy samples are etched for 2 minutes using a Keller's solution, and then cleaned using water, ethanol, and finally dried by compressed air. An XJP-3A microscope (Figure 3-18, left) is used for optical microscopy; it is equipped with a Clemex video camera which allows the images to be transferred to a computer. Scanning electron microscopy samples are coated with gold (Au) or silver (Ag) to increase the conductivity of the specimens during SEM investigations. Scanning electron microscopy investigations are performed using a ZEISS electron microscope (SEM EVO-MA10, Zeiss, Germany) (Figure 3-18, right) equipped with an Energy dispersive X-ray spectroscopy (EDX) detector (INCA-x-act, Oxford Instruments, Abingdon-Oxfordshire, UK) for chemical analysis. Optical and scanning electron microscopy investigations allow exploring sample microstructures, chemical composition, phase formation at the interface, defect identification, and porosity. A quantitative evaluation of the porosity at interfaces is completed using an optical microscope and the image analysis software Clemex Vision lite 0.6. Image analysis is done at 400X magnification; the light gray areas are identified as carbon fiber, the dark areas as porosity and the remaining bright zone as the matrix as seen in Figure 3-17.

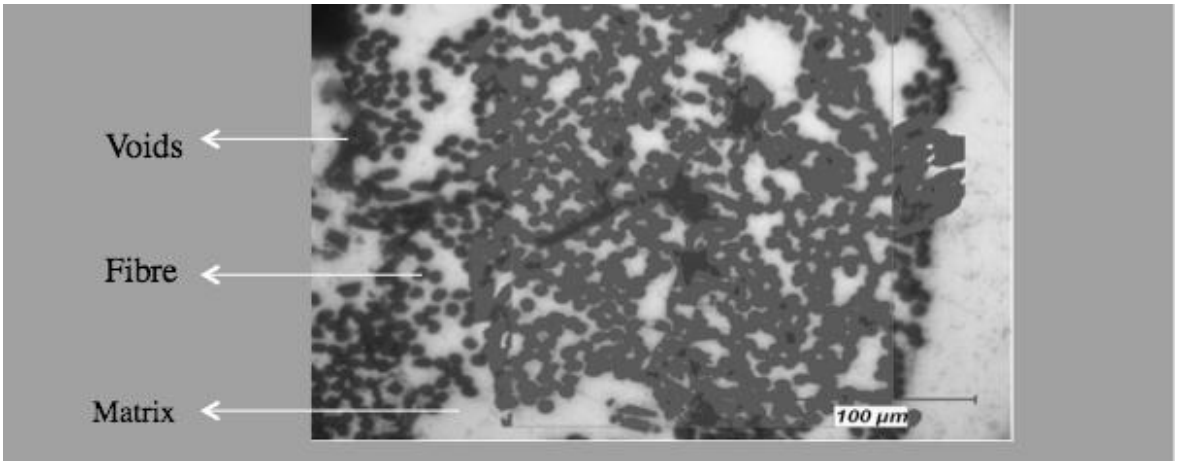

Figure 3-17: Image analysis of porosity at the carbon fiber/aluminium matrix interface.

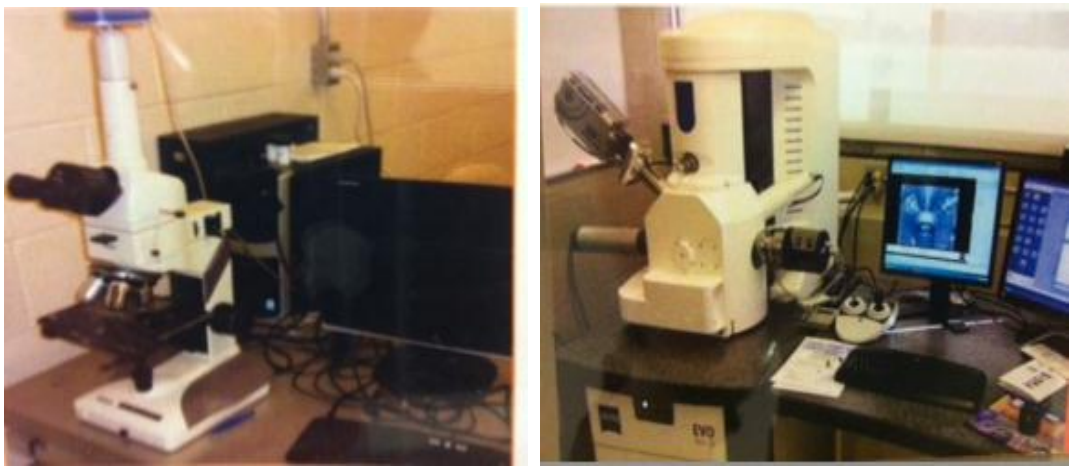

Figure 3-18: XJP-3A optical microscope (left) and ZEISS electron microscope (right) used for microscopic analyses.

4 RESULTS

4.1 Sample references and configuration

Different compositions, configurations and carbon fiber volume fractions are investigated as shown in Table 4.1. The laminate sequences are presented in the format of [NF/C] where F represents an aluminium foil layer; N represents the number of foils in the respective layer; C_1 and C_2 represent a carbon fiber fabric layer as received and after removal of every second yarn respectively. Each sequence as shown in Table 4.1 represents from left to right the order of aluminium foils and fabric layers from the top to the bottom of the laminate. The carbon fiber volume fraction for each laminate composite is calculated using equation (4.1) [23] and is also provided in Table 4.1.

$$v_{f(\%)} = \left[\frac{\left(\frac{\rho_f}{w_f}\right)\times N}{V_c}\right] \times 100 \tag{4.1}$$

Where ρ_f is the fabric carbon fiber density; w_f is the fabric carbon fiber weight; N is the number of plies; and V_c is the composite specimen volume.

Table 4.1: Investigated sample references, configurations, carbon fiber volume fractions, and sample specificities.

Sample Ref.	Configuration	(v_f) %	Specificities
S_1	[2F/C_1/2F/C_1/2F/C_1/2F/C_1/2F]	14.117	Stainless steel foil used as shim in fabrication
S_2	[2F/C_1/2F/C_1/2F/C_1/2F/C_1/2F]	13.997	Stainless steel foil used as shim in fabrication
S_3	[5F/C_2/2F/C_2/2F/C_2/2F/C_2/5F]	7.080	Stainless steel foil used as shim and modified plate used on one side in fabrication
S_4	[5F/C_2/2F/C_2/2F/C_2/2F/C_2/5F]	7.402	Modified plates used in fabrication
S_5	[5F/C_2/2F/C_2/2F/C_2/2F/C_2/5F]	7.213	Modified plates used in fabrication
S_6	[5F/C_2/2F/C_2/2F/C_2/2F/C_2/5F]	9.642	Modified plates used in fabrication
S_7	[5F/C_1/2F/C_1/2F/C_1/2F/C_1/5F]	13.498	Modified plates used in fabrication
A_1	6061/1235-H19 aluminium	-----	Fabricated by squeeze casting

4.2 Microstructural evaluation and chemical composition

Microstructural analysis of each sample in Table 4.1 was carried out using Optical Microscopy (OM) and Scanning Electron Microscopy (SEM). Optical microscopy is used to characterize casting structure and to quantitatively assess the porosity at the fiber/matrix interface, while SEM is used to evaluate the fiber/matrix interface, chemical composition, and precipitation of new phases at grain boundaries. The objective of this section is to elucidate the dependence of the microstructure on the manufacturing variables that are mainly carbon fiber volume fraction and composition.

4.2.1 Optical microscopy analyses of fiber/matrix interface

The typical SEM micrograph of S_4 is shown in Figure 4-1 that illustrates the matrix boundary between two laminates of plain weave. The matrix boundaries of all samples differ in shape and show variations in laminate plies interspacing. These variations in laminate shape and distance between fabric plain weaves are affected by variations in sample preparation and carbon fiber volume fraction.

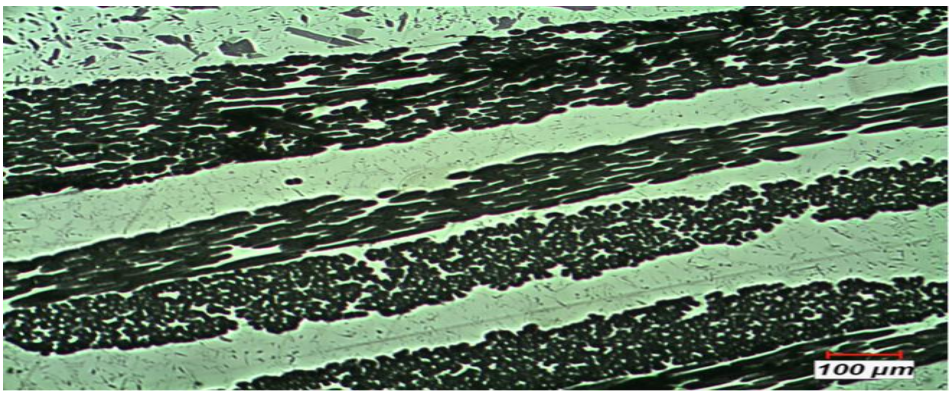

Figure 4-1: SEM Micrograph of S_4 sample showing matrix and carbon fiber ply laminates.

A quantitative evaluation of the porosity at interfaces is completed for all samples. Also, a statistical quantitative evaluation is done to calculate the percentage of the porosity at the interface in each sample. It is found that the inter-diffusion between carbon fibers and matrix contributes to better interface bonding and to lower porosity at the interface as can be seen in Figure 4-2.

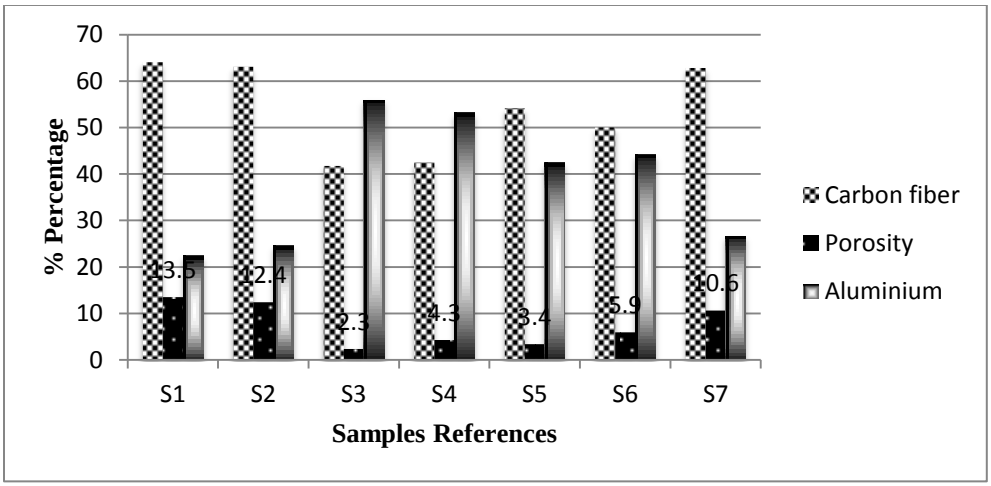

Figure 4-2: Percentages of carbon fiber, porosity and aluminium at the carbon fiber/aluminium matrix interface.

4.2.2 Scanning electron microscopy analyses and chemical composition

Area chemical analysis using EDX (Energy-Dispersive X-Ray Spectroscopy) is performed as shown in Figure 4-3. It shows that alloying of elements takes place at the interface. Also, element percentages at the interface vary between samples as shown in Table 4.2.

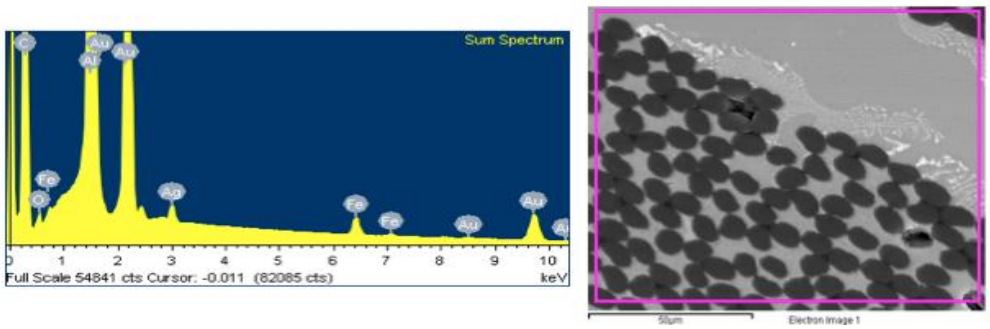

Figure 4-3: EDX map (right), and diffraction pattern of elemental mapping (left).

Table 4.2: Elemental weight percentages and chemical compositions of the different samples as measured using EDX mapping.

	S_1	S_2	S_3	S_4	S_5	S_6	S_7
Elements	**Content in weight %**						
Al	16.28	27.19	35.08	31.96	47.09	31.76	13.45
C	81.15	70.20	62.87	65.92	48.70	66.14	83.77
Fe	0.16	0.17	1.34	0.59	1.92	0.40	0.17
O	2.41	2.44	0.71	1.32	1.51	1.70	2.61
Cr	--	--	--	0.12	0.54	--	--
Ni	--	--	--	0.09	0.24	--	--
Total	100	100	100	100	100	100	100

It is obvious from Table 4.2 that the basic elements are aluminium, carbon, oxygen and iron. Between the different samples, the weight percentages of aluminium and carbon range from 13.45 to 47.09wt% for aluminium, and 48.70 to 83.15wt% for carbon. Some precipitates are also observed at grain boundaries as can be seen in Figure 4-4. The results of EDX analysis are provided in Figure 4-5 and Table 4.3. The main characteristic of the precipitates is that they contain about 4.3wt% iron, which is a much higher concentration than in the aluminium matrix. The size and the shape of precipitates vary between samples S_1 , S_2 , S_3 , S_6 and S_7.

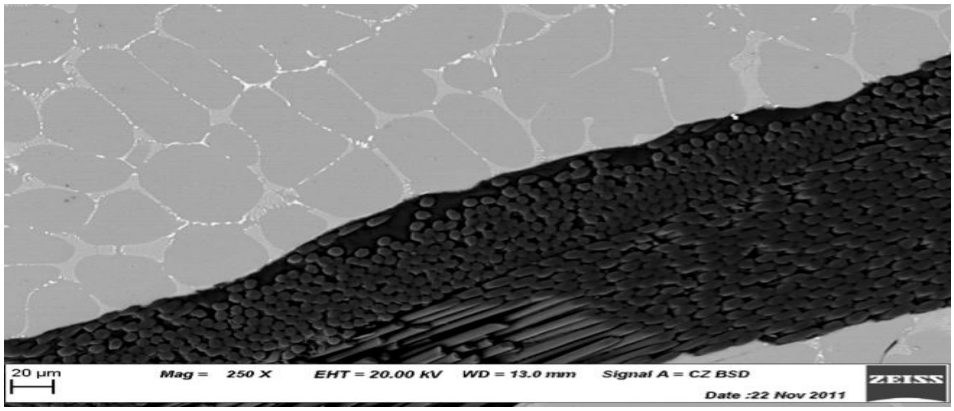

Figure 4-4: Elongated precipitates at matrix grain boundaries in sample S_1.

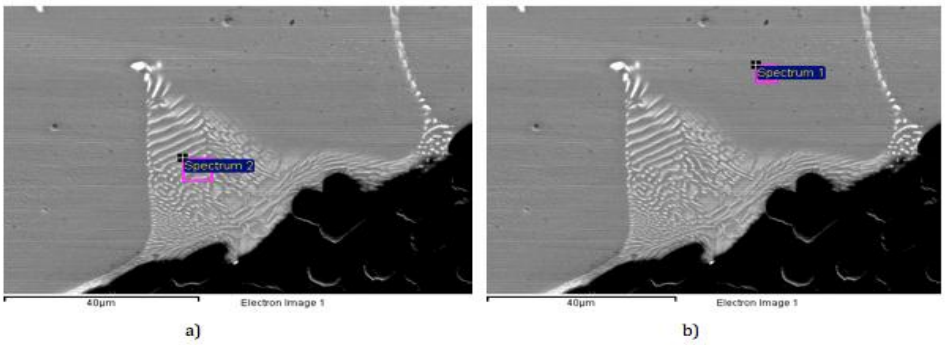

Figure 4-5: EDX spectra a) at precipitate, and b) at the matrix.

Table 4.3: Element concentrations at grain boundaries and in the matrix.

	Matrix	**Precipitate**
Elements	**Content in weight %**	
C	4.73	3.92
Al	93.93	90.47
O	1.34	1.31
Fe	0	4.31
Total	100	100

Figure 4-6 b, c and d show the variation of element concentrations along the line across matrix, interface and carbon fiber shown in a.

A second class of precipitates is found in some samples S_4 and S_5 as shown by arrows in Figure 4-7; they are blocky in shape and appear brighter than the first type of precipitates. Gaunt and area mapping shows that this second type of precipitates are rich in chromium, iron and nickel as illustrated in Table 4.2.

A higher concentration of carbon is observed in the aluminium matrix as a result of carbon diffusion from fibers. As illustrated in Figure 4-8, matrix carbon concentrations of about 5.84% are observed.

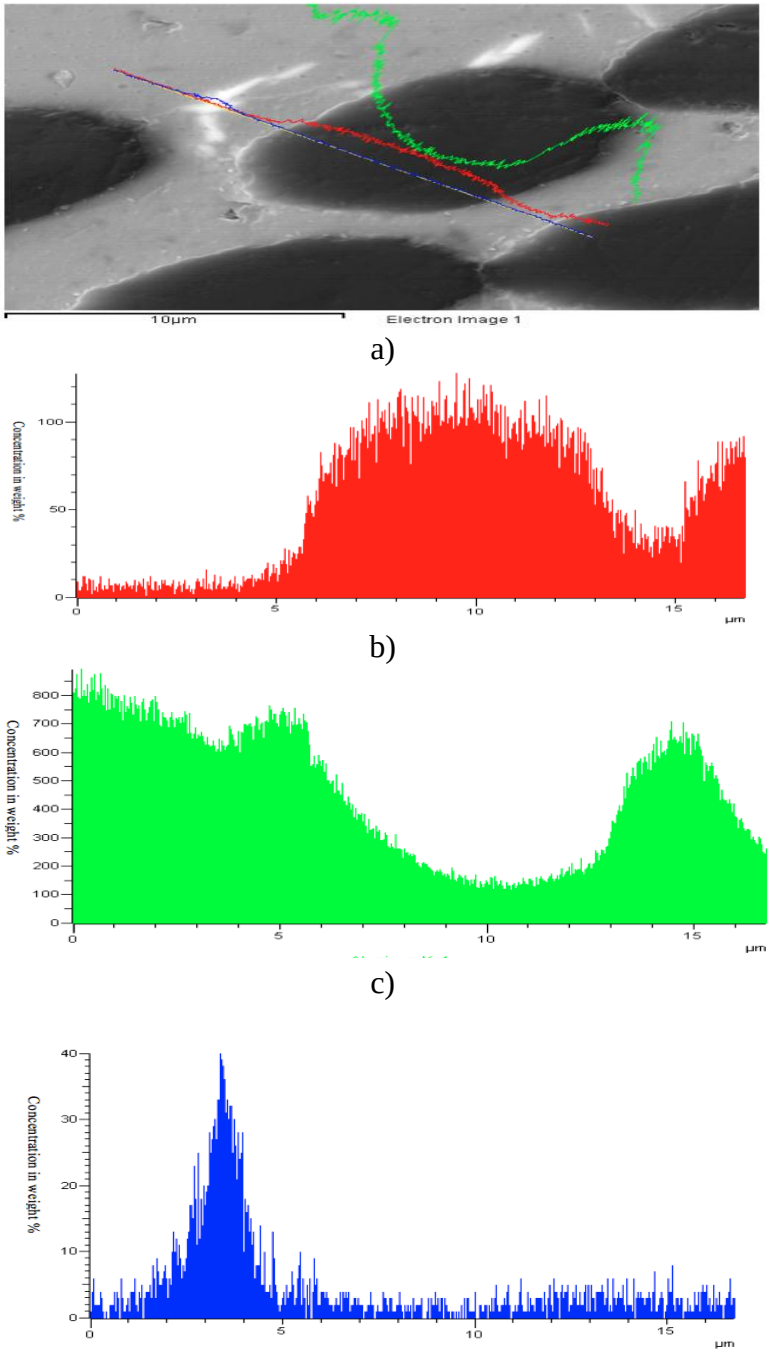

Figure 4-6: a) SEM-EDX line map across matrix, interface and carbon fiber in sample S_6: element distribution for b) carbon, c) aluminium, and d) iron along the mapped line.

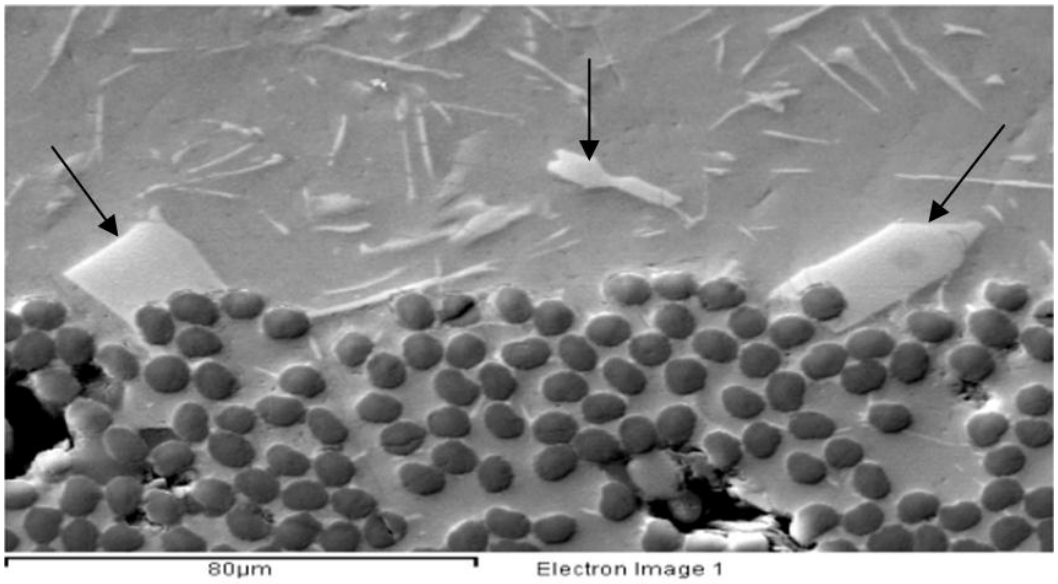

Figure 4-7: Blocky precipitates in samples S_4 and S_5.

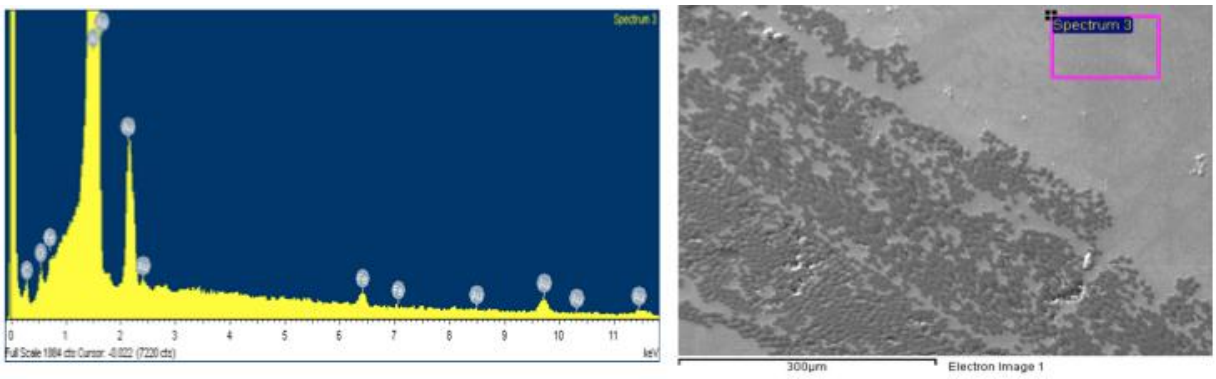

Figure 4-8: EDX area mapping of the matrix (right) and resulting diffraction pattern (left).

Figure 4-9 and Table 4.4 provide the result of EDX area mapping for 6061/1235-H19 aluminium alloy A_1 fabricated by squeeze casting which is the reference alloy used in this study. Similar to composites and as illustrated in Table 1.4, 4.01wt% of carbon is also observed in A_1 due to carbon interdiffusion from the die materials and the graphite lubricant. A_1 also shows some precipitates at grain boundaries. Figure 4-10 and Table 4.5 show tentative measurement results of the chemical composition of these precipitates.

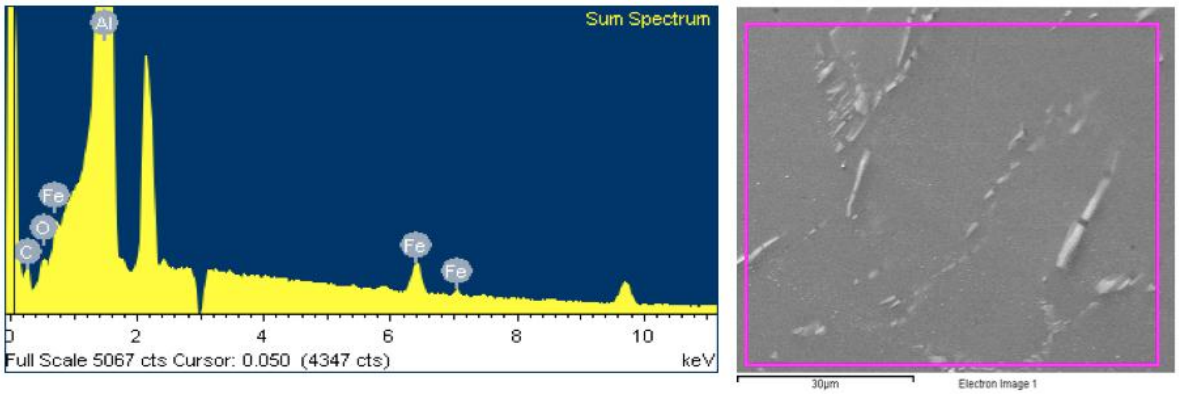

Figure 4-9: EDX area mapping showing the chemical analysis of the reference alloy A_1.

Table 4.4: Chemical composition of 6061/1235-H19 aluminium alloy (A_1) fabricated by squeeze casting.

	A_1
Elements	**Contents in weight %**
C	4.01
Al	94.21
O	0.85
Fe	0.93
Mn	--
Total	100

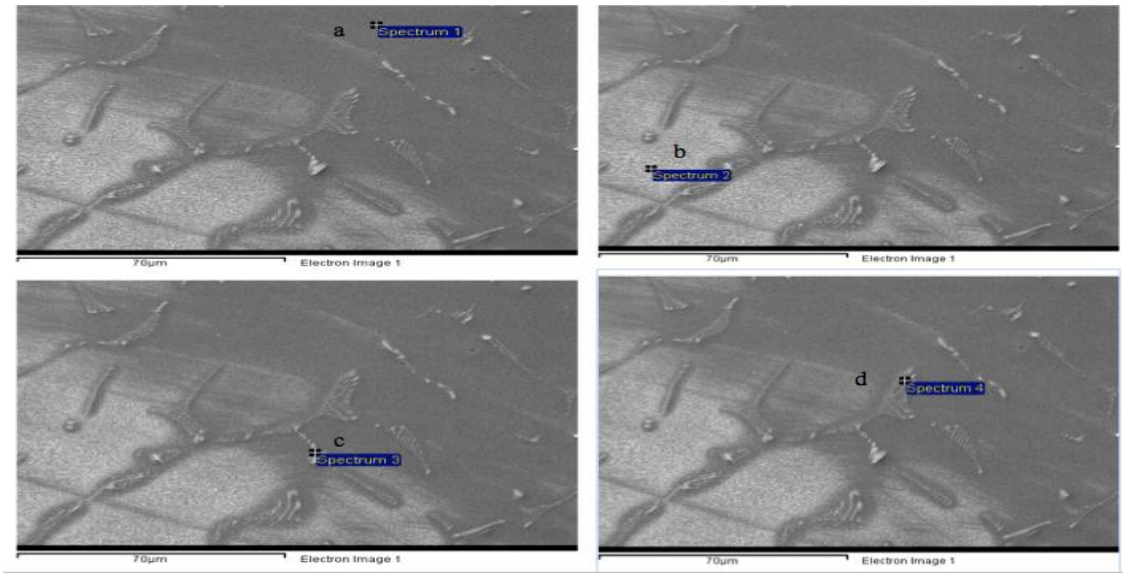

Figure 4-10: Gaunt map analysis for element concentrations at precipitates in the base aluminium alloy A_1.

Table 4.5: Element weight percentages in grain boundary precipitates in the base 6061/1235-H19 aluminium alloy fabricated by squeeze casting.

	A_1			
Elements	**Contents in weight %**			
	a	**b**	**c**	**d**
Al	93.50	93.86	68.43	91.07
C	5.98	4.87	4.91	5.75
Fe	--	--	18.81	3.18
O	0.51	1.27	--	--
Si	--	--	--	--
Ni	--	--	1.87	--
Mn	--	--	0.43	--
Cu	--	--	0.51	--
Total	100	100	100	100

4.3 Hardness

Results of Vickers hardness measurements are summarized in Figure 4-11; samples S_4 and S_5 have the highest carbon fiber/aluminium matrix interface hardness while samples S_1 and S_7 show the lowest hardness. The matrix Vickers hardness of S_4 and S_5 is also the highest while the matrix of all other samples are lower and statistically comparable with that of the base aluminium matrix alloy (see Figure 4-11). Figure 4.11 also shows that the fiber/matrix interface is almost 2.5 times harder than the matrix.

At macro scale, at least ten indentation measurements were done at different locations in composite specimens, and the averages plotted in Figure 4-12. It shall be noted that smaller indentation diameters mean higher material resistance to indentation and therefore higher

hardness. It can again be seen that S_4 and S_5 are harder than all other composites and the 6061/1235-H19 aluminium reference alloy.

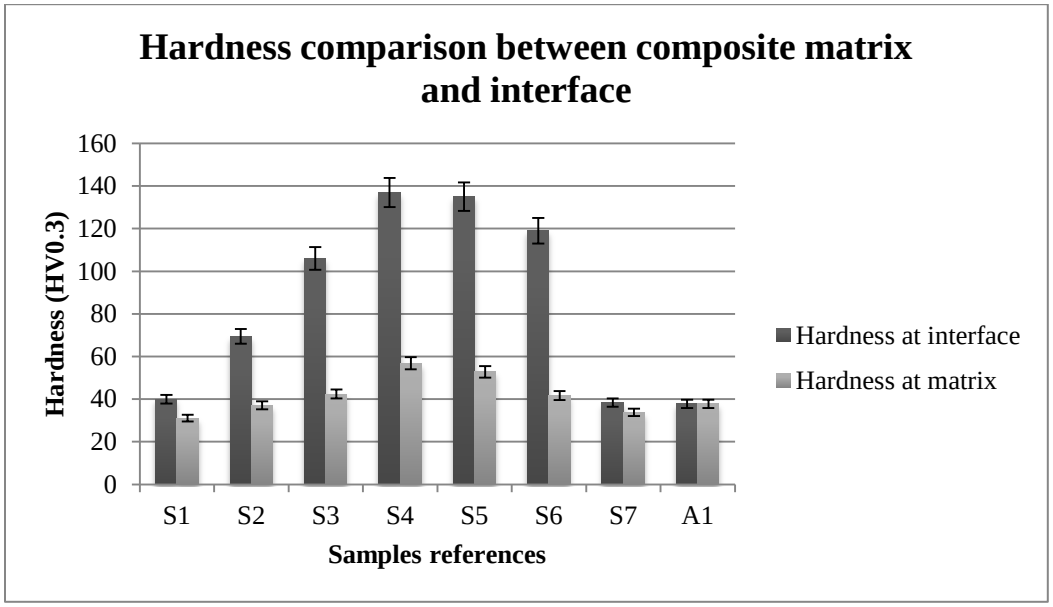

Figure 4-11: Hardness comparison between composite matrix, carbon fiber/matrix interface and 6061/1235-H19 aluminium reference alloy.

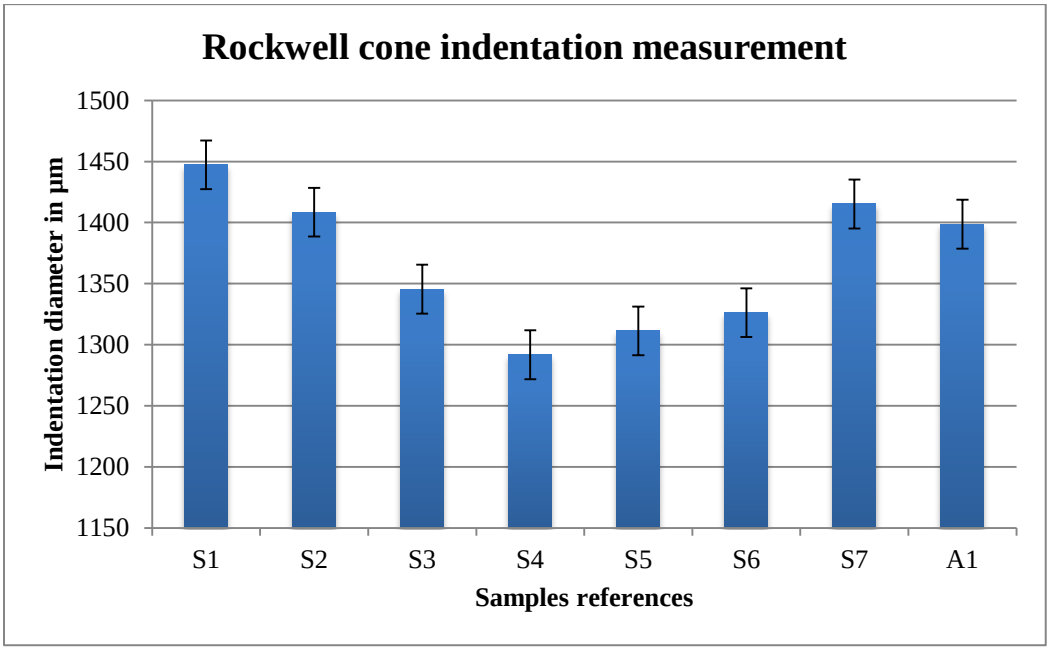

Figure 4-12: Rockwell cone indentation diameter measurement (bulk hardness) for the different composite samples and the 6061/1235-H19 aluminium reference alloy.

4.4 Bend resistance

Figure 4-13 shows the load-deflection curves during bend tests for all investigate samples. The bend resistance is highest for S_3, S_4, S_5, S_6 and S_7 while S_1, S_2 exhibit low bend resistance in the same range as that of the base aluminium alloy. Figure 4-14 illustrates the assessment of the initial elastic proportionality according to the linear trend equation provided in the diagram as the initial slop of the load-deflection curves and the bend moduli; estimated bend modulus values are provided in Table 4.6.

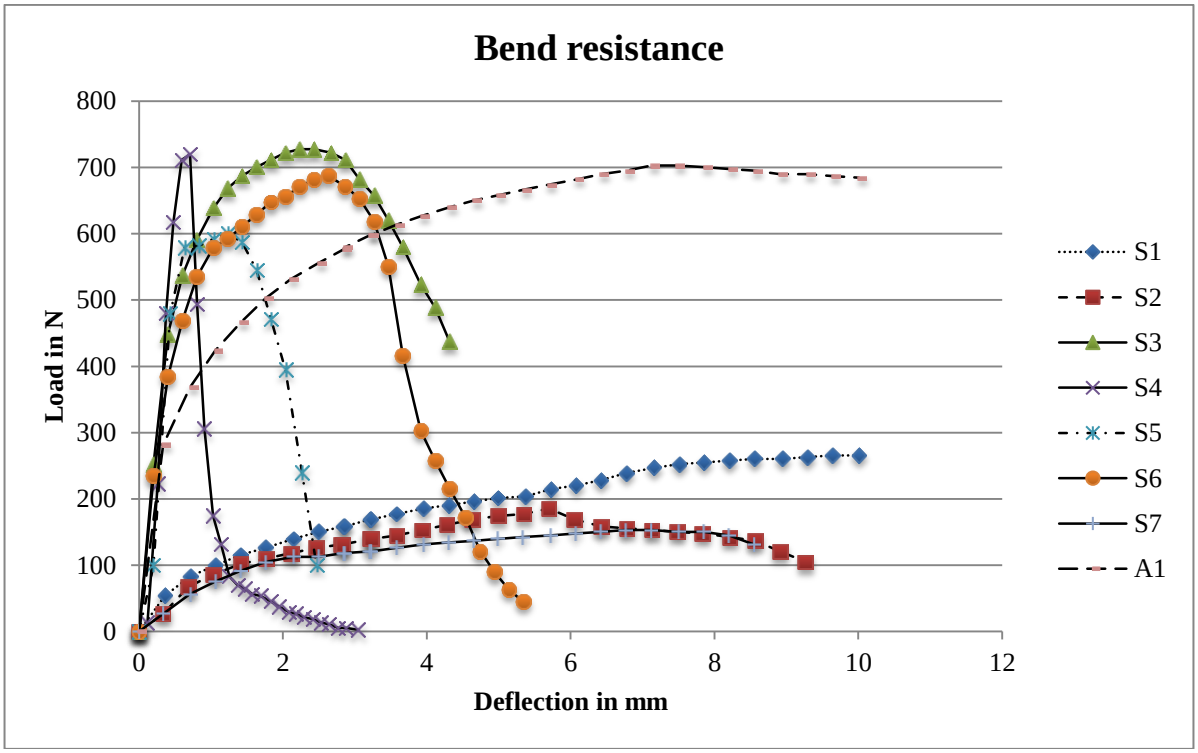

Figure 4-13: Load versus deflection curves for three point bend test.

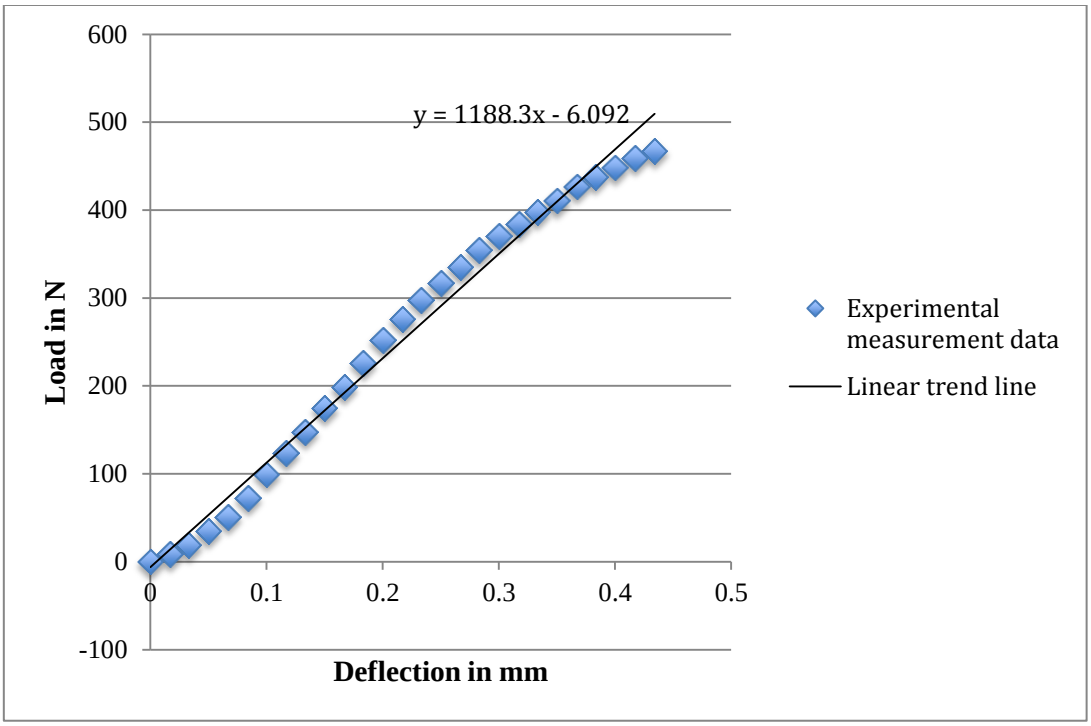

Figure 4-14: Estimate of the initial elastic proportionality and bend modulus.

Table 4.6: Sample dimensions and bend moduli for the different composites and the 6061/1235-H19 aluminium reference alloy.

Samples	Thickness d (mm)	Length L (mm)	Width b (mm)	m (P/D)	E (GP)
S_1	3.49	40	12	182.58	5.73
S_2	3.52	40	12	132.95	4.06
S_3	4.52	40	12	1188.3	17.12
S_4	4.33	40	12	1662	27.36
S_5	4.44	40	12	1378.1	20.99
S_6	4.34	40	12	1107.5	18.02
S_7	3.65	40	12	85.584	2.35
A_1	4.34	40	12	959	15.64

4.5 Impact energy absorption

The energy absorbed (E_{abs}) during impact test as well as their thickness specific values (energy divided by the thickness) are presented in Table 4.7. Overall, 6061/1235-H19 aluminium alloy absorbs the most energy and is tougher than all composites.

Table 4.7: Impact energy absorbed during Charpy impact test.

Samples	Thickness (mm)	E_{abs} (J)	I (J/mm)
S_1	3.49	3.4	0.97
S_2	3.52	3	0.85
S_3	4.52	9.3	2.06
S_4	4.33	7.7	1.78
S_5	4.44	6.3	1.42
S_6	4.34	7.6	1.75
S_7	3.65	3	0.82
A_1	4.34	11.6	2.67

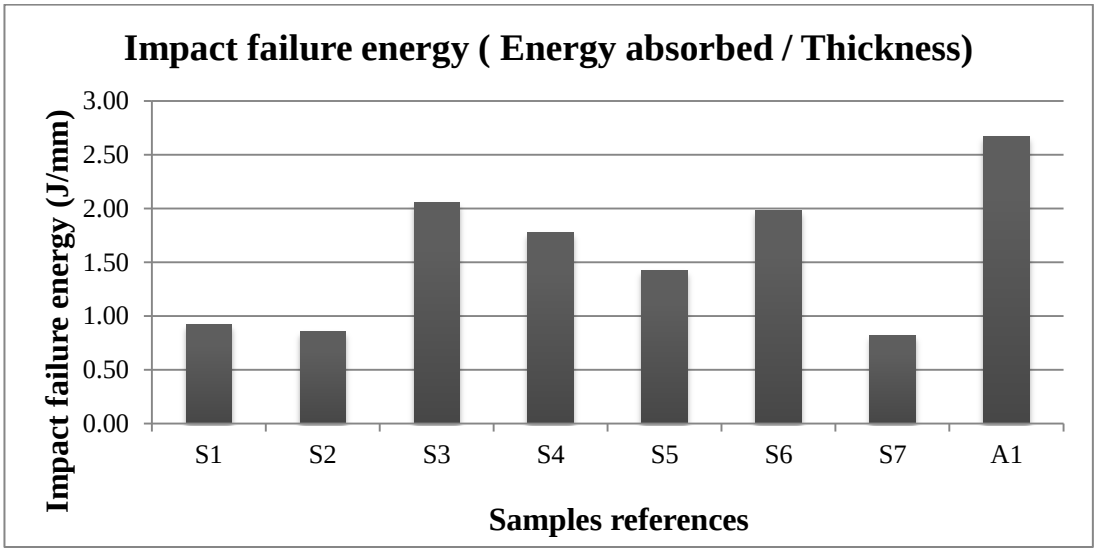

Figure 4-15: Impact fracture energy during Charpy impact test for all composites and for 6061/1235-H19 aluminium reference alloy.

A visual qualitative assessment is done by evaluating the fracture mode for each sample as shown in Figure 4-16. As can be observed, the fracture mode differs from sample to sample. An estimation of percentages of ductile and brittle fracture modes is illustrated in Table 4.8.

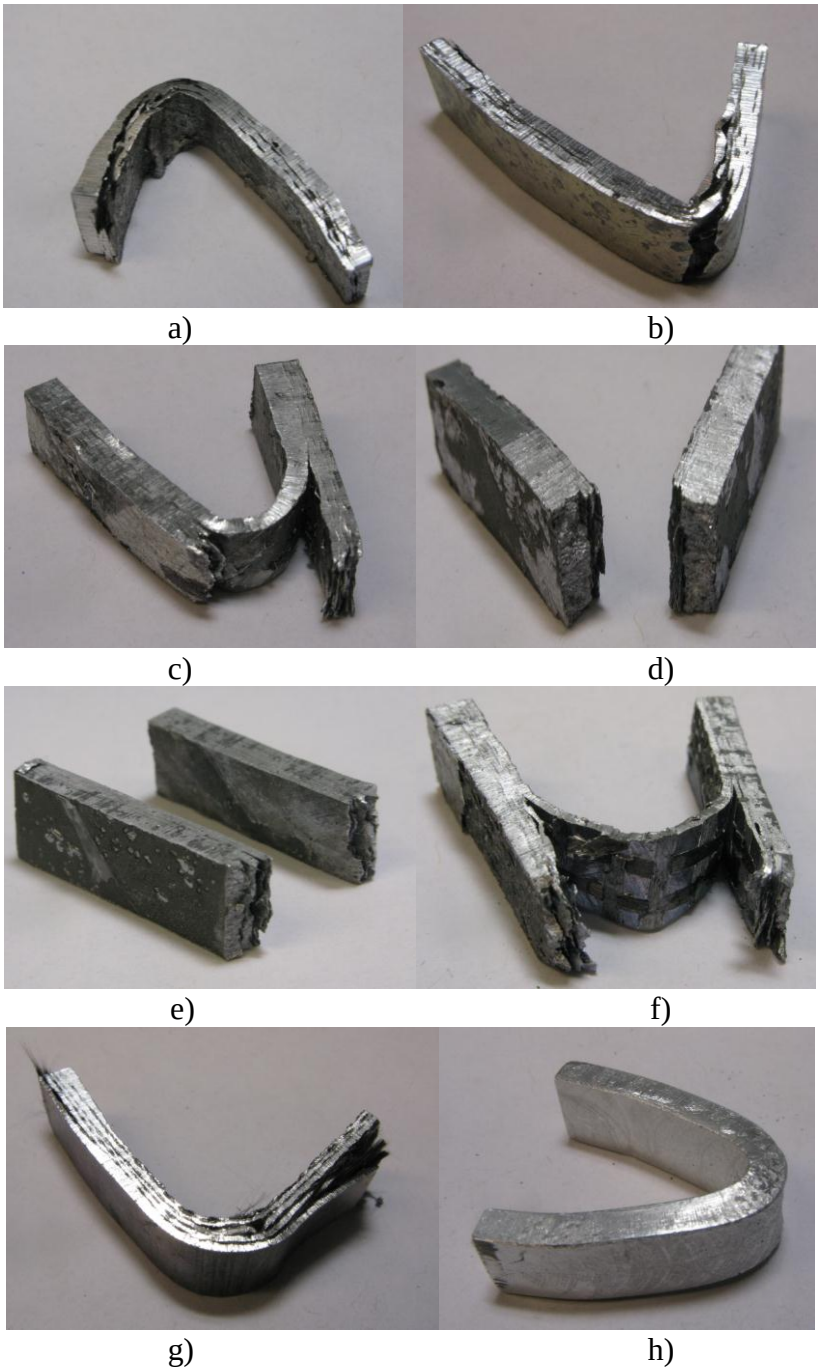

Figure 4-16: Nature of fracture and fracture modes of composites and 6061/1235-H19 aluminium reference alloy during impact test: a) S_1; b) S_2; c) S_3; d) S_4; e) S_5; f) S_6; g) S_7; h) A_1.

Table 4.8: The fracture modes for each sample based on visual investigation and percentage for each failure mode.

Samples	Fracture modes	Percentage %	Comments
S_1	Ductile - interlaminar	100%	Delamination due to weak carbon fiber/aluminium matrix interface bond
S_2	Ductile - interlaminar	100%	Delamination due to weak carbon fiber/aluminium matrix interface bond
S_3	Brittle - ductile (mixed fracture)	50-50%	Partial fracture through matrix and fiber + fiber/matrix delamination
S_4	Brittle	100%	Matrix embrittlement due to carbon diffusion into the matrix
S_5	Brittle - interlaminar	70-30%	Partial fracture through matrix and fiber + fiber/matrix delamination
S_6	Brittle	100%	Matrix embrittlement due to carbon diffusion into the matrix
S_7	Ductile - interlaminar	80-20%	Partial fracture through matrix and fiber + fiber/matrix delamination
A_1	Ductile	100%	Ductility of pure aluminium with some participation

5 DISCUSSION

5.1 Fiber/matrix adhesion

The adhesion between the fiber and the matrix plays an important role in different ways. The first bonding mechanism is mechanical and is achieved by pressurizing molten aluminium [48] to 20 MPa. Bonding through liquid pressurizing is due to interlocking of the aluminium matrix with the single fiber and with carbon fiber preform as a whole. This bonding mechanism can be described as wetting between the solid fiber surface and liquid aluminium. Wetting and surface tension are determined by the contact angle as can be seen in Figure 5-1. The squeeze pressure is used to reduce the contact angle as close as possible to zero to improve wetting and fiber/matrix bond. The relationship between contact angle and surface tension is described by the Young's equation as [49]:

$$\gamma_{SG} = \gamma_{SL} + \gamma_{LG}\, cos\theta_c \tag{5.1}$$

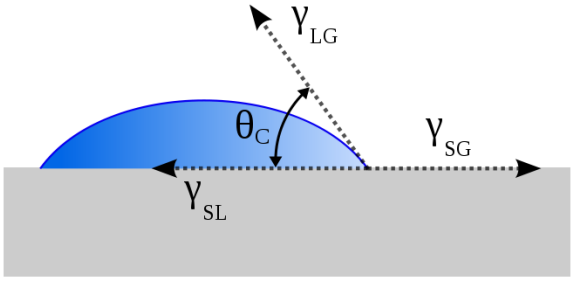

Figure 5-1: Schematic illustration of the contact angle between solid and liquid phases.

The second bonding mechanism is chemical. Chemical reaction between aluminium and carbon takes place at 500°C resulting in heterogeneous formation of aluminium carbide (Al_4C_3) at the interface [32] as proven using TEM microscopy [49]:

$$4\ Al + 3\ C \rightarrow Al_4C_3 \tag{5.2}$$

Figure 5-2 shows aluminium atom and carbon atom positions during new crystal nucleation.

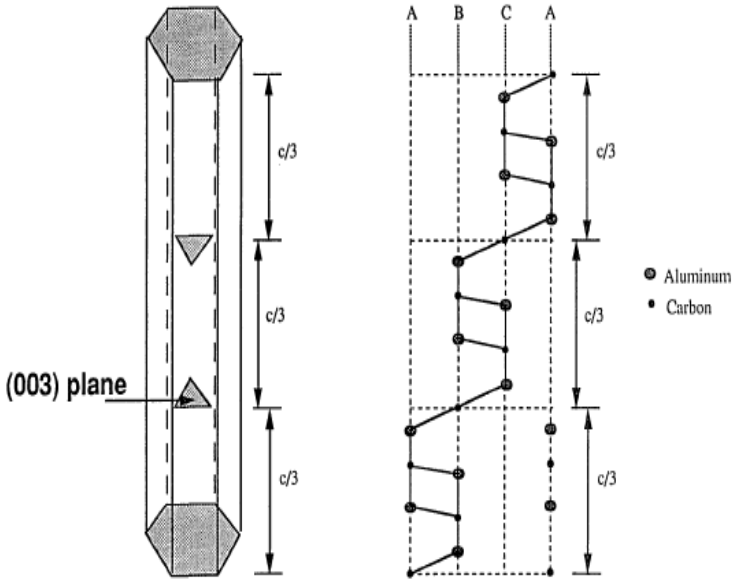

Figure 5-2: Al_4C_3 during new crystal nucleation [49].

Precipitates are observed using EDX at fiber/matrix interfaces as bright color interlayers. It has been shown that an increase in carbon concentration at carbon fiber aluminium matrix interface can be linked to the formation of aluminium carbides as observed in S_3, S_4, S_5, and S_6 samples. The formed Al_4C_3 phase is relatively brittle which leads to low impact fracture energy and to brittle fracture during Charpy impact tests. In addition to fibers, carbon from the die graphite lubricant and from the steel die can diffuse into the aluminium matrix leading to heterogeneous chemical composition throughout the composite matrix. Moreover, the presence of oxygen in the furnace during heating of the carbon fiber/aluminium laminate and melting of aluminium leads to oxidation and to the formation of a potentially Al_4O_4C phase at the interface which can further affect fiber/matrix bonding [50]. Aluminium reaction with oxygen and carbon

at the interface can also produce Al_4C_3 and carbon monoxide (CO) according the equation (5.3) below. CO is a toxic gas and can cause pores at the interface [51].

$$2\ Al_2O_3 + 9\ C \rightarrow Al_4C_3 + 6\ CO \tag{5.3}$$

Overall, the presence of oxygen can be detrimental to the composites. Using an inert environment can help prevent oxidation during squeeze casting, eliminate oxides at the interface and improve the quality of the composites.

5.2 Precipitates at matrix grain boundaries

Two types of precipitates are observed at the composite grain boundaries. (1) Elongated precipitates appear in S_1, S_2, S_3, S_6 and S_7 samples. They are iron rich with their chemical composition varying amongst samples. They are thought to be iron aluminides (Fe_3Al) created by iron diffusion from the die into the molten aluminium during squeeze casting. (2) Blocky precipitates are found in S_4 and S_5. They are rich in chromium, iron and nickel. Chromium and nickel emanates from the 1235-H19 aluminium foils, while iron primarily emanates from the die during casting. The reference aluminium sample also contains some precipitates as listed in Table 4.2. These precipitates are rich in carbon, iron and nickel. Again, iron and carbon obviously emanate from the die and the graphite lubricant during casting, while nickel comes from the 6061 aluminium alloy used as starting material for sample manufacture. Some oxide formation is found as well in the pure aluminium sample.

5.3 Viscosity versus temperature and effect on the composites quality

One of the important variables that affect the quality and the bond between fiber and matrix of the composites is the viscosity of the molten aluminium. During squeeze casting, the

aluminium viscosity depends on temperature as can be seen in Figure 5-3. Viscosity decreases with increasing temperature which favours liquid flow around carbon fiber, and improves wettability between the matrix and the fiber. In this work, the temperature of aluminium melt is 850°C. This temperature seems to achieve good viscosity, wetting and bonding as can be seen in the Results chapter.

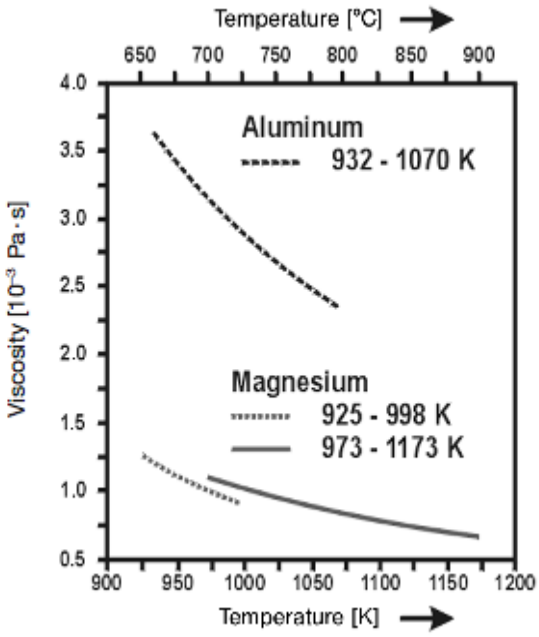

Figure 5-3: Effect of temperature on the viscosity of aluminium [51].

Further increasing the squeeze casting temperature could lead to better results due to even lower liquid viscosity. However, increased temperature also means more oxidation of aluminium foils and sheets which could lead to increased oxide content between the laminates and consequently to poor inter-laminar bond.

5.4 Impact of carbon fiber volume fraction

The carbon fiber volume fraction plays an important role for composite strengthening and stiffness. Based on the mathematical rule of mixture, an increase in carbon fiber volume fraction

can be expected to improve mechanical properties [25]. However, the results of this thesis indicate that there is an optimum fiber volume fraction that provides best mechanical properties. For example, it can be seen that with regard to hardness and flexural modulus, S_4 with a fiber volume fraction of 7.402% yields best results while other samples with either lower or higher fiber volume fractions show lower performance.

Fiber volume fraction and distribution have also been found to affect fiber/matrix bond. Increased carbon fiber volume fraction leads to more restricted flow of the molten aluminium and to stronger pressure drop during squeeze casting, and consequently to higher porosity, decreased interlocking and weaker fiber/matrix bond in the final composite. For example, S_1, S_2 and S_7 samples have higher fiber volume fraction and microscopy results show that their fibers are less wetted by the matrix; some loose fibers are observed as well in these samples. Also, more homogeneous distribution of the fibers leads to stronger bond, while heterogeneous fiber distributions lead to more areas of excessive fiber concentrations and consequently to more locations of weaker fiber/matrix bond. For example, S_3, S_4, S_5 and S_6 have more homogeneous fiber distributions that result in a stronger mechanical bond. Higher hardness values of S_3, S_4, S_5 and S_6 could be linked both to stronger fiber/matrix bond and to substantially higher flexural strength of the composite.

The carbon fiber volume fraction also affects the bond strength between the fiber and the matrix. Figure 5-4 describes the behaviour of the liquid infusion into the fiber with varying fiber content [52]. It has been proven both mathematically and experimentally that with increasing carbon volume fraction the liquid flow resistance increases and the permeability decreases. In this work, Figure 5-5 shows the effect of carbon volume fraction on the porosity of the composite. This plot demonstrates that with increasing carbon volume fraction there are more

regions where the matrix does not infused the carbon fiber fabric properly resulting in porosity at the interface between the fibers and the aluminium matrix. The increased porosity at the fiber/matrix interface favours debonding and degrades mechanical properties due to the deterioration of load transfer capacity between matrix and fibers. For instance, S_1, S_2 and S_7 with higher carbon volume fraction show lower mechanical properties compared to S_3, S_4, S_5 and S_6 as described in the Results chapter.

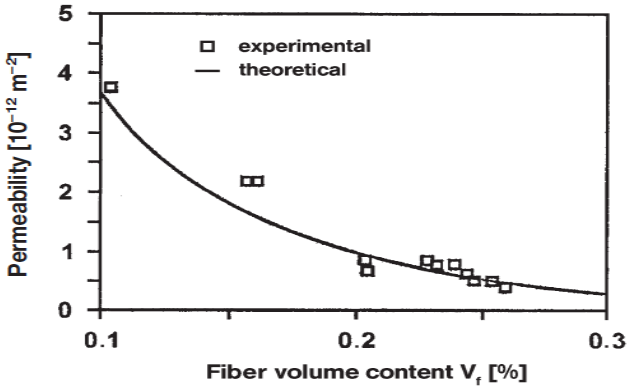

Figure 5-4: Liquid infusion into fibers as a function of fiber volume content [52].

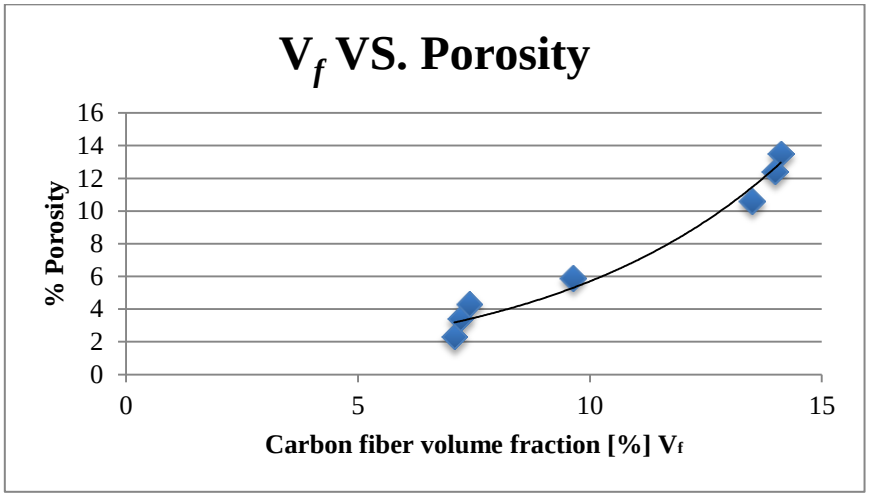

Figure 5-5: Effect of carbon fiber volume fraction on composite porosity.

5.5 Manufacturing defects

Although manufacturing the composites is done successfully, some manufacturing difficulties and defects are observed and partly solved. First, the pressurized molten aluminium

leaked out between the die and the plunger which made it difficult to maintain the required pressure. Using stainless steel foils as envelopes to contain the molten aluminium liquid solved this problem at the initial stage. However, this solution caused high levels of contamination in the composites. Also, the drop in temperature of the sample-die assembly during its transfer from the furnace to the squeeze press as well as the fast cooling of die and samples once in contact with the cold press base and the punch contributed to deteriorate the fluidity and the impregnation capacity of the molten aluminium. Adding two pre-heated stainless steel flat plates of 1 cm thickness in the die, one below and one on top of the sample, successfully solved this premature sample cooling problem. The pre-heated plates allowed maintaining the required temperature before and during squeezing of the specimens. Furthermore, plates and die are lubricated using a dry graphite lubricant (DOALL) in order to prevent adhesion and sticking of the composite samples to the die, to the steel plates and to the plunger, as well as to facilitate sample ejection from the die after squeeze casting.

6 CONCLUSIONS

Carbon fiber/aluminium matrix composite laminate plates are successfully manufactured by squeeze-casting technique using carbon fiber fabric, aluminium sheets and foils. The fabricated composites show the following microstructure and mechanical properties.

I. There is a good adhesion bond between the fiber and the aluminium matrix; this bond is achieved both (1) mechanically through good fiber wetting by molten aluminium and (2) chemically through carbon and aluminium interdiffusion and reactions at the carbon fiber/aluminium matrix interfaces during casting.

II. The hardness of the composites is improved by over 50% at macro and micro scales compared to the reference 6061/1235-H19 aluminium alloy squeeze casted under identical conditions.

III. The flexural strength and modulus of the composites increase by about 55% compared to that of the reference 6061/1235-H19 aluminium alloy squeeze casted under identical conditions.

IV. The toughness of the composites decreases compared to the reference 6061/1235-H19 aluminium alloy squeeze casted under identical conditions due to either (1) the presence of brittle phases such as in samples S_3, S_4, S_5 and S_6, in which case the composite toughness can be improved by better oxidation prevention; or (2) fiber/matrix debonding (delamination) such as in samples S_1, S_2 and S_7.

V. There seems to be an optimal fiber volume fraction at which the properties are best, i.e. maximum hardness, stiffness and toughness are achieved.

Overall, the present work successfully demonstrates a new fabrication method for aluminium matrix composite plates by squeeze casting technique using laminates of aluminium sheets/foils

and carbon fiber fabric. The fabricated composites show potentially better properties than the reference 6061/1235-H19 aluminium alloys. This provides the basis for future research and development of gradient composite materials as well as novel combinations of fiber and ceramic particulate/dispersion strengthening.

7 OUTLOOK

The current work has only focused on fabricating aluminium matrix composite laminate plates by squeeze casting technique using aluminium sheets/foils and carbon fiber as reinforcement. The following suggests future work that can potentially further advance research and development of carbon fiber aluminium matrix composites made by squeeze casting:

- Reducing oxidation, for instance by using an inert environment such as vacuum could substantially improve the properties of the resulting composites. Also, pre-melting and skimming the molten aluminium before pouring it into the pre-heated die already containing pre-heated carbon fiber fabric and then immediately squeezing could substantially reduce oxidation, oxide formation at fiber/matrix interfaces and consequently substantially improve composite properties.
- Further mechanical properties evaluation is needed such as using tensile, compression, fatigue and creep tests.
- The effect of fiber orientation on composite properties has to be investigated.
- The effect of thermal post-processing heat treatment on the composite microstructure and properties has to be studied.
- Accurately determining the optimal fiber volume fraction could help further optimize composite properties as well.
- Finding ways to better seal the die-plunger assembly during squeeze casting could allow to further increase the squeeze pressure; improve liquid flow, wetting and bonding between carbon fiber and aluminium matrix; improve load transfer between matrix and fibers; and ultimately produce better composite strength and toughness.

REFERENCES

[1] D. Miracle, "Metal Matrix Composites – From Science to Technological Significance," Composites Science and Technology, vol. 65, no. 15-16, pp. 2526-2540, 2005.

[2] A. Evans, C. Marchi, and A. Mortensen, Metal Matrix Composites in Industry: An Introduction and a Survey, Dordrecht, Netherlands: Kluwer Academic Publisher, 2003.

[3] I. A. Ibrahim, F. A. Mohamed, and E. J. Lavernia, "Particulate Reinforced Metal Matrix Composites," Journal of Materials Science, vol. 26, no. 5, pp. 1137-1156, 1991.

[4] N. Gupta, K. G. Satyanarayana, and C. Materials, "Symposium Review: Solidification Processing of MMCs," Journal of Materials Science, vol. 58, no. 11, pp. 91-93, 2006.

[5] ASM Handbook, Casting, vol. 15, ASM International, 1996.

[6] T. W. Chou, A. Kelly, and A. Okurat, "Composites de Matrices en Métal Renforcés aux Fibres", Composites, vol. 16, no. 3, pp. 183-184, 1985.

[7] A. Kelly, S. Fishman, and A. Dhingra, "Metal Matrix Composite, A Review," In Proceeding International Symposium on Advances in Cast Reinforced Metal Composite, Chicago, USA, 1988.

[8] J. K. Wessel, The Handbook of Advanced Materials, New Jersey, USA: John Wiley & Sons Inc., 2004.

[9] W. Callister, and D. Rethwisch, Materials Science And Engineering: An Introduction, 8th ed., New Jersey, USA: John Wiley & Sons Inc., 2003.

[10] L. Froyen, and B. Verlinden, "Aluminium Matrix Composite Materials," EAA-European Aluminium Association, pp. 1-28, 1994.

[11] J. Kaczmar, "The Production and Application of Metal Matrix Composite Materials," Journal of Materials Processing Technology, vol. 106, No.1-3, pp. 58-67, 2000.

[12] T. Vijayaram, S. Sulaiman, A. Hamouda, and M. Ahmad, "Fabrication of Fiber Reinforced Metal Matrix Composites by Squeeze Casting Technology," Journal of Materials Processing Technology, vol. 178, no. 1-3, pp. 34-38, 2006.

[13] T. Shalu, E. Abhilash, and M. A. Joseph, "Development and Characterization of Liquid Carbon Fibre Reinforced Aluminium Matrix Composite," Journal of Materials Processing Technology, vol. 209, no. 10, pp. 4809-4813, 2009.

[14] ASM Handbook, Powder Metal Technologies And Applications: Conventional Aluminium Powder Metallurgy, vol. 7, ASM International, 1998.

[15] P. R. Roberge, Corrosion Basics: An Introduction, 2nd ed., Houston, USA: NACE Press Book, 2006.

[16] S. V. Hoa, Principles of the Manufacturing of Composite Materials, 1st ed., Pennsylvania, USA: DEStech Publications Inc., 2009.

[17] C. Science, and K. A. Publishers, "Carbon Fibers for Composites," Journal of Materials Science, vol. 5, pp. 1303-1313, 2000.

[18] S. C. Bennett, D. J. Johnson, and W. Johnson, "Strength-Structure Relationships in PAN-Based Carbon Fibres," Journal of Materials Science, vol. 18, no. 11, pp. 3337-3347, 1983.

[19] NRC, High-Performance Synthetic Fibers for Composites, Publication NMAB-458, Washington, D.C., USA: National Academy Press, 1992.

[20] J. B. Donnet, and R. C. Bansa, Carbon Fibers: In Polymers for Advanced Technologies, 2nd ed., New York, USA: Marcel Dekker, 1992.

[21] G. M. Jenkins, and K. Kawamura, Polymeric Carbons, 1st ed., London, UK: Cambridge University Press, 1976.

[22] L. A. Dobrzañski, M. Kremzer, A. J. Nowak, and A. Nagel, "Aluminium Matrix Composites Fabricated by Infiltration Method," Archives of Materials Science and Engineering, vol. 36, no. 1, pp. 5-11, 2009.

[23] F. Robitaille, "Introduction to Composite Materials," Class lecture, Faculty of Engineering, University of Ottawa, Ottawa, Ontario, Nov. 2010.

[24] V. F. Okhuysen, "A Practical Assesment of Fiber Reinforced Aluminium Matrix Composites", Materials Processing Technology, vol. 3, pp. 235-265, 2004.

[25] T. Shalu, E. Abhilash, and M. A. Joseph, "Development and Characterization of Liquid Carbon Fibre Reinforced Aluminium Matrix Composite," Journal of Materials Processing Technology, vol. 209, no. 10, pp. 4809-4813, 2009.

[26] C. S. Lim, and Clegg, "The Production and Evaluation of Metal-Matrix Composite Castings Produced by a Pressure-Assisted Investment Casting Process," Journal of Materials Processing Technology, vol. 67, pp. 13-18, 1997.

[27] B. D. Agarwal, and L. J. Broutman, Analysis and Performance of Fiber Composites, 2nd ed., New York, USA: John Wiley and Sons Inc., 1990.

[28] T. L. Richardon, and E. Lokensgard, Industrial Plastics: Theory and Application, 3rd ed., New York, USA: Delmar Cengage Learning, 1989.

[29] C. M. Friend, "The Effect of Matrix Properties on Reinforcement in Short Alumina Fibre-Aluminium Metal Matrix Composites," Journal of Materials Science, vol. 22, no. 8, pp. 3005-3010, 1987.

[30] B. Wielage, "Corrosion Studies on Aluminium Reinforced with Uncoated and Coated Carbon Fibres," Composites Science and Technology, vol. 59, no. 8, pp. 1239-1245, 1999.

[31] M. Lancin, "TEM Study of Carbon Fibre Reinforced Aluminium Matrix Composites: Influence of Brittle Phases and Interface on Mechanical Properties," Journal of the European Ceramic Society, vol. 20, no. 10, pp. 1493-1503, 2000.

[32] V. Scott, R. Trumper, and M. Yang, "Interface Microstructures in Fibre-Reinforced Aluminium Alloys," Composites Science and Technology, vol. 42, no. 1-3, pp. 251-273, 1991.

[33] S. Kalpakjian, and S. R. Schmid, Manufacturing Engineering Technology. 5th ed., New Jersey, USA: Pearson Education Inc., 2005.

[34] E. Hajjari, M. Divandari, and A. R. Mirhabibi, "The Effect of Applied Pressure on Fracture Surface and Tensile Properties of Nickel Coated Continuous Carbon Fiber Reinforced Aluminum Composites Fabricated by Squeeze Casting," Materials & Design, vol. 31, no. 5, pp. 2381-2386, 2010.

[35] B. C. A. Vogel, and R. D. Doherty, "Stir-Cast Microstructures and Slow Growth," In Proceeding Conference on Solidification and Casting of Metals, 1977.

[36] A. N. A. El-Azim, M. A. Kassem, Z. M. El-Baradie, and M. Waly, "Structure and Properties of Short Alumina Fibre Reinforced AlSi18CuNi Produced by Stir Casting," Materials Letters, vol. 56, pp. 963-969, 2002.

[37] J. Hashim, "Metal Matrix Composites: Production by The Stir Casting Method," Journal of Materials Processing Technology, vol. 92-93, no. 1, pp. 1-7, 1999.

[38] S. Naher, D. Brabazon, and L. Looney, "Development and Assessment of a New Quick Quench Stir Caster Design for The Production of Metal Matrix Composites," Journal of Materials Processing Technology, vol. 166, no. 3, pp. 430-439, 2005.

[39] S. Prabu, L. Karunamoorthy, S. Kathiresan, and B. Mohan, "Influence of Stirring Speed and Stirring Time on Distribution of Particles in Cast Metal Matrix Composite," Journal of Materials Processing Technology, vol. 171, no. 2, pp. 268-273, 2006.

[40] J. Torralba, "P/M Aluminum Matrix Composites: An Overview," Journal of Materials Processing Technology, vol. 133, no. 1-2, pp. 203-206, 2003.

[41] A. N. Palazotto, and R. Run, "Introduction to Metal Matrix Composites in Aerospace Application," American Society of Civil Engineering ASCE, vol. 1, no. 1, pp. 3-17, 1988.

[42] D. Lloyd, "Particle Reinforced Aluminium and Magnesium Metal Matrix Composite Materials," Metal Powder Report, vol. 49, no. 9, p. 50-58, 1994.

[43] M. Taya, "Strengthening Mechanisms of MMCs," Materials Transactions, vol. 32, pp. 1-19, 1990.

[44] H. Chen, and A. T. Alpas, "Wear of Aluminium Matrix Composites Reinforced with Nickel-Coated Carbon Fibres," Wear, vol. 192, no. 1-2, pp. 186-198, 1996.

[45] N. R. Baddoo, and B. A. Burgan, "Structural Design of Stainless Steel," The Steel Construction Institute, pp. 55-62, 2001.

[46] R. W. Hertzberg, Deformation and Fracture Mechanics of Engineering Materials, 4th ed., New York, USA: Wiley Inc., 1996.

[47] A. P. Boresi, R. J. Schmidt, and O. Sidebottom, Advanced Mechanics of Materials, 6th ed., New York, USA: John Wiley & Sons Inc., 1993.

[48] T. S. Chow, "Wetting of Rough Surfaces," Journal of Physics: Condensed Matter, vol. 10, pp. 445-453, 1998.

[49] A. P Diwanji, Interface Characterization of Carbon/Aluminum Composite, Ph.D. Thesis, University of Delaware, 1990, pp. 73-78.

[50] H. Nayeb-Hashemi, and J. Seyyedi, "Study of Interface and its Effect on Mechanical Properties of Continuous Graphite Fiber-Reinforced 201 Aluminum," Metallurgical and Materials Transactions, vol. 20, pp. 727-732, 1989.

[51] P. Balomenos, F. Paspaliaris, S. Jaroni, H. Guglielmini, and V. Epstein, "Carbothermic Reduction of Alumina, A Review of Developed Processes and Novel Concepts," In Proceeding Conference of EMC, 2011.

[52] A. Mortensen, and T. Wong, "Infiltration of Fibrous Preforms by a Pure Metal," Part III. , Metallurgical and Materials Transactions, vol. 21, pp. 2257–2263, 1990.